May 2015

Investigation of Distributed Model Predictive Control for Economic Load Shifting in Building HVAC Systems

Peter Kinsella
University of Wisconsin-Milwaukee

INVESTIGATION OF DISTRIBUTED MODEL PREDICTIVE CONTROL FOR ECONOMIC LOAD SHIFTING IN BUILDING HVAC SYSTEMS

by

Peter A. Kinsella

A Thesis Submitted in

Partial Fulfillment of the

Requirements for the Degree of

Master of Science

in Engineering

at

The University of Wisconsin-Milwaukee

May 2015

ABSTRACT

INVESTIGATION OF DISTRIBUTED MODEL PREDICTIVE CONTROL FOR ECONOMIC LOAD SHIFTING IN BUILDING HVAC SYSTEMS

by

Peter A. Kinsella

The University of Wisconsin-Milwaukee, 2015
Under the supervision of Professor Yingchun Yuan

One of the major challenges that building owners and operators face is maintaining a low cost of operation. In certain markets within the U.S., electrical cost varies throughout the day; it is higher during times of peak demand. This leaves the customer the incentive to cut back electrical use during peak demand periods. Since 40% of the peak electrical demand is due to the operation of the building HVAC system alone, the opportunity exists for shifting the building cooling load to off-peak hours. This can be done by pre-cooling the space, thereby using the building mass as a sort of thermal battery, which can then discharge later, alleviating the cooling load off the HVAC system during peak times. It is in this thesis that a peak load reduction strategy is presented using model predictive control (MPC). Furthermore, the system modeled in this paper is a two-zone system, each having a dedicated controller. First the problem is explored with a single, centralized MPC which calculates the optimal trajectory for the entire building. Secondly, the load reduction strategy control is distributed to each individual controller. The advantage to distributed control is the reduction of computing resources which brings with it a cost reduction on its own. Lastly, both MPC approaches are

compared to the traditional PI-only control scheme. Results showed that the distributed scheme proved favorable next to the centralized MPC benchmark, and both MPC approaches produced favorable results over the traditional PI-only control.

TABLE OF CONTENTS

LIST OF FIGURES

LIST OF FIGURES CONTINUED

LIST OF TABLES

LIST OF ABBREVIATIONS

DR	Demand Response
HVAC	Heating, Ventilation & Air Conditioning
IAQ	Indoor Air Quality
LTI	Linear, Time-Invariant
LQR	Linear Quadratic Regulator
MIMO	Multi-Input, Multi-Output
MIN	Minimum
MPC	Model Predictive Control
ODE	Ordinary Differential Equation
PI	Proportional plus Integral
PID	Proportional plus Integral plus Derivative
RTO	Real-time optimization
RTU	Rooftop Unit
SISO	Single Input, Single Output
TOU	Time of Use

LIST OF SYMBOLS

A	System Matrix
B	Input Matrix
C	Output Matrix
D	Direct Feed-through Matrix
x(t)	State variable vector
u(t)	Output from controller to the plant
y(t)	Plant output
G_p	Transfer function representing plant dynamics
G_c	Transfer function representing controller
H(s)	Transfer function representing sensor dynamics
J	Cost Function or Performance Index
K	State feedback gain matrix

Chapter 1: Problem Introduction

1.1 Motivation

Reducing building energy use and the associated cost, is a major challenge currently facing building owners and operators. In 2010, the U.S. aggregate electrical utility cost of commercial buildings alone reached nearly $135 billion. Making up the single largest portion of this was the operation of building HVAC systems, which accounted for $49 billion. Projecting into 2035, electrical utility spend when adjusted for inflation, is expected to rise steadily. For a Real GDP growth at an annual rate of 2.4%, electrical demand is estimated to increase from 3,826 billion kWh in 2012 to 4,954 billion kWh in 2040 [1]. Actual electricity demanded will depend on enhancements of energy efficiency technologies, economic growth and electricity prices. Uncertainty around forecasting such demand growth will impact capacity additions on the supply side as well.

A critical balance between electrical supply and demand must be maintained for the sake of a reliable and stable transmission grid [2]. This presents a challenge for the power generation company. Electrical demand by end users tends to strengthen synchronously within a predictable timeframe over a 24-hour period. If at any point during the day, generation capacity is unable to keep up with electrical demand, power transmission to the end users will be unreliable. On the other hand, adding electrical generation capacity in excess of demand is not cost effective, since storage

of excess electricity generated is not practical [2]. This means building power plants to satisfy demand peaks lasting a few hours during the day is economically inefficient. Therefore, the decision by the power company to add generation capacity must consider the initial costs and the uncertain future demand.

An economically feasible solution that the utility has is the ability to charge prices for electrical use that are in line with electrical demand. Historically, the cost of electricity charged to the end user has been on a flat-rate basis. However, recent technological advancements in smart metering infrastructure enable the utility to measure electrical use in real-time, thereby enabling price increases to be charged to the customer during peak periods [3]. Consumers are effectively incentivized to reduce electrical usage during periods of peak demand; otherwise they bear the true cost of electricity production during peak hours. The opportunity for leveling out electricity production throughout the day becomes possible, and power generators don't have to rely on costly investments in power generation capacity and infrastructure for the purpose of meeting peak demands lasting a few hours of the entire day.

On the demand side, consumers are afforded the option to reduce their electrical consumption at peak periods of the day or shift a certain amount of their demand to off-peak hours. The practice of altering normal electrical consumption patterns on the demand side in response to time-varying pricing or incentive payments designed to curtail loads is commonly referred to as demand response. There is

flexibility in how incentives are structured to motivate demand response participation. Programs are either classified as time-based or incentive-based. Specifically, time-based programs are those where the price of electricity varies over the course of a day. A time-of-use (TOU) rate is charged to customers for use of electricity during certain blocks of time in a given 24-hour period. The pricing reflects the actual cost of electrical generation during those blocks of time. A real-time-pricing (RTP) rate is charged to customers on an hourly basis, and the cost represents the wholesale cost of electricity in a given hour. Customers who enroll in the RTP option are notified of pricing by the day-ahead or sometimes hour-ahead of when prices take effect. Then, there is a structure referred to as critical peak pricing (CPP). In this structure, the default pricing is time-of-use; however, the peak price is replaced by the critical peak price. Triggering of the critical peak price occurs when grid reliability is threatened, or the cost of supplying electricity is exceptionally high.

Incentive-based demand reduction programs are contractual agreements between the utility and customers which provide for payments to customers from the utility for committing to load curtailments during system contingencies. On the other hand, penalties may be levied for non-compliant customers when signaled to reduce loads. Programs vary according to the degree of load reduction. Direct load control allows a program operator to directly cycle customer's electrical equipment on a last-minute notice. This sort of program is reserved for mostly residential and light commercial customers. Larger customers may (1MW or over) be offered to

participate in a bid/buy-back program. In this type of program, the customer bids on curtailment based on wholesale electricity prices. The largest electrical customers are offered interruptible/curtailable service where a rate discount or bill credit is provided for those entities agreeing to curtail loads during system contingencies. In this program, a penalty may be charged against those not reducing loads.

The Federal Energy Regulatory Commission assessed the demand response potential in the U.S. and published its findings per the Energy Independence and Security Act of 2007. The top ten states assessed to have the highest potential for peak demand reduction are shown in Figure 1 [4].

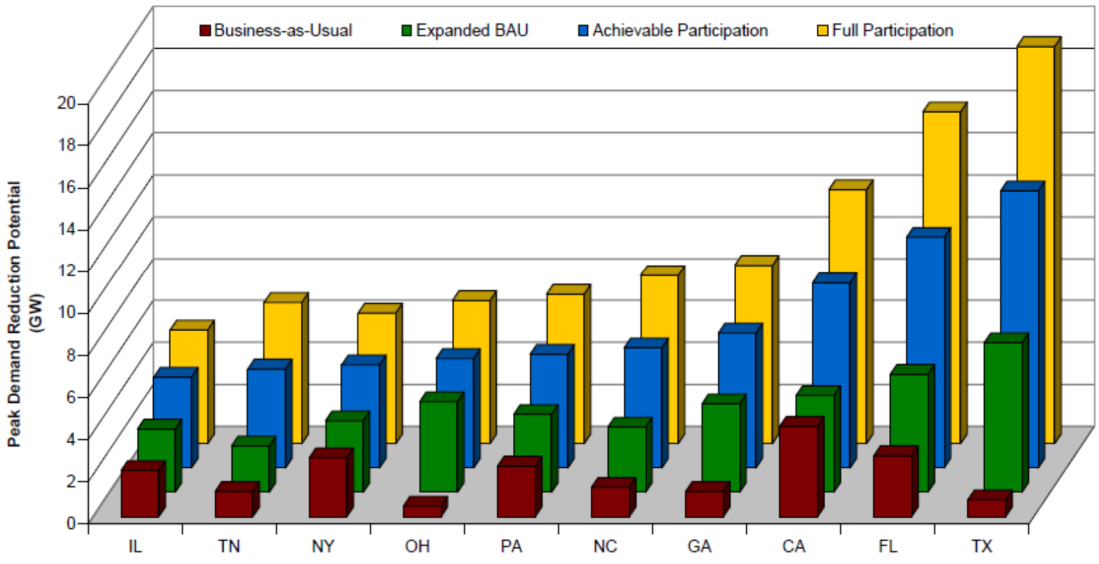

Figure 1 - Assessment of U.S. States with highest achievable potential by 2019 (GW). Source: Federal Energy Regulatory Commission, 2009.

Each of the four cases considered represents a set of assumptions about factors that influence the demand response potential. The business-as-usual (BAU) case is simply the estimated demand response potential given current practices. It serves as a benchmark for comparison to the other three scenarios. The expanded business-as-usual case represents the current mix of demand response programs expanded to all states with a participation rate equal to the 75th percentile of participation rates of existing programs of the same type and customer class. Achievable participation refers to the estimate of demand response potential that could likely be achieved in reality. In this scenario, it is presumed that advanced metering infrastructure is universally deployed, and alternative pricing methods are available for those customers not opting in to the dynamic pricing as a default. The full participation scenario assumes that all customers actively participate in a demand response program. It provides a quantitative estimate of the upper bound of demand response potential.

Customers who opt to participate in demand response will choose to reduce their peak loads in a way that makes sense for them. Some of the common strategies include shifting business hours one to two hours earlier in the day, shutting off lighting in unoccupied areas of the building, and allowing the temperatures in the occupied space to slide to the minimum level of comfort by shutting down components of the HVAC system. Shifting the hours of business one to two hours earlier in the day allows less usage of lighting, computers and the building HVAC system during the peak afternoon hours. However, consideration must be given for

employees' schedules and the overall impact to the business from shifting operations to non-traditional hours [3]. Lighting may be managed by shutting off lights in unoccupied areas of the building, and the use of occupancy sensors enables automation in lighting throughout the day, regardless of peak or off-peak hours. Additionally, the building HVAC system is identified as a promising load shedding opportunity, especially in regions where there is a high use of central air conditioning systems [4]. It is estimated that the HVAC system alone accounts for 40% of the building's peak electrical demand [5]. Hence, a considerable potential exists for load shedding via control of the HVAC system.

Load shedding of the HVAC system may be accomplished by shifting the peak load to off-peak periods. Because the energy efficiency of heating systems and the per unit energy cost (natural gas or oil) do not vary with time, the most significant opportunities for cost savings are derived from shifting cooling loads as opposed to shifting heating loads [6]. The on-peak cooling load is mitigated with the pre-cooled building mass. Typically, the internal gains are 3-7 W, with 70% of these gains in the form of electromagnetic radiation directly absorbed by the internal surfaces before being transmitted to the air space via convection [6]. Considering that the thermal capacity of building structures is about 3.6 – 7.2 W-h/°C, the potential for shifting peak cooling loads to off-peak periods is significant [6].

One other method is setting the temperature setpoints to their absolute edges of the comfort zone during peak periods; however, the thermal mass of the building is not

leveraged. Therefore, setpoints may not be maintained without staging on the full cooling capacity to meet the peak cooling load, thus costing extra money.

Shifting the peak cooling load from the HVAC system is performed by running the system at max capacity during off-peak hours to pre-cool the space prior to shutting down during the peak period. For example, during the summertime, cooling of the space would occur in the hours leading up to a load curtailment event. During this time, the temperatures in the space will likely reach their lower acceptable bounds. When the point of load shed begins, the pre-cooled mass of the building will keep the zone temperature comfortable until HVAC systems are cycled back on at the end of the load curtailment period. If a system has to be brought on early to keep the zone temperature from rising too high, less energy is used during the on-peak period because of the pre-cooling that took place during the off-peak period. The amount of load shifting depends on the characteristics of the building, occupant behavior and weather conditions.

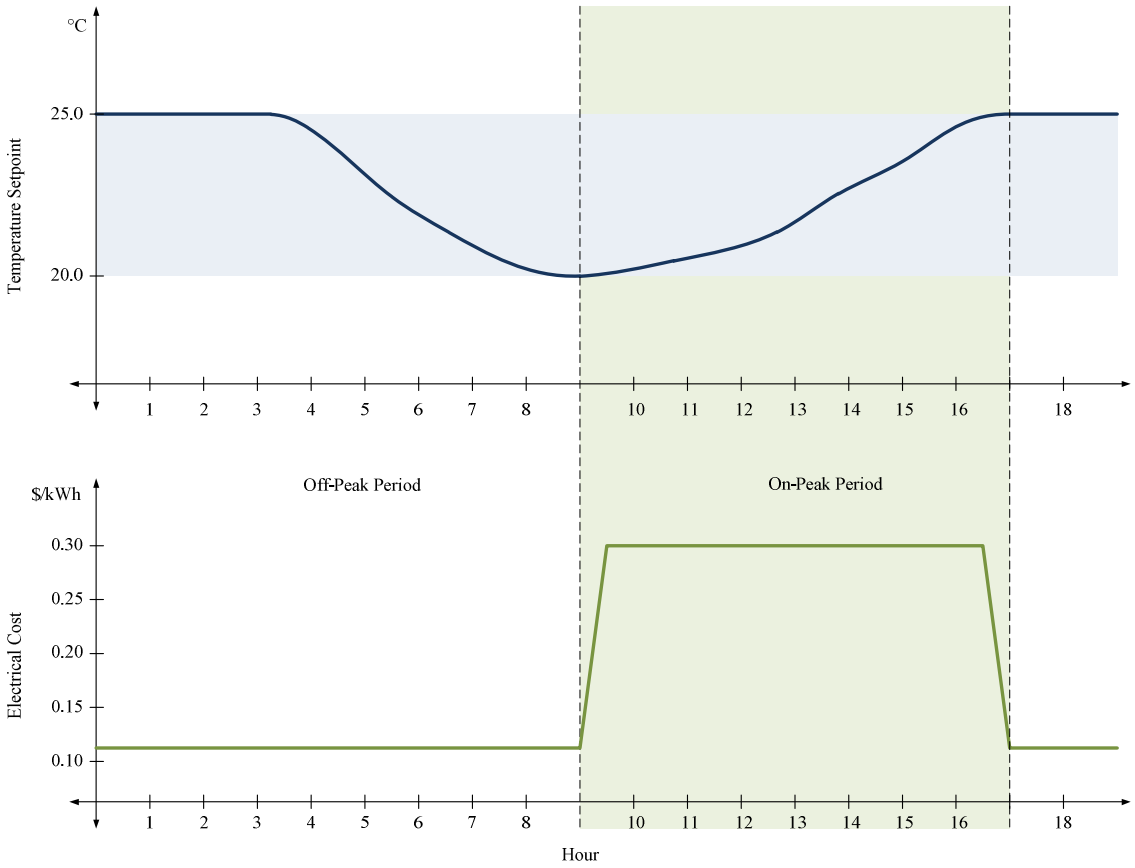

Figure 2 – Load shifting by optimally pre-cooling the space prior to electrical price hike

1.2 Air-Side HVAC Systems Background

An occupied space is conditioned with some version of an air-handling unit. A rooftop unit (RTU) is designed with commercial purpose in mind. It's mounted on a roof curb, saving premium commercial real estate for more profitable uses. The RTU is a packaged version of the air-handling unit, which means all equipment and controls are in one unit without additional installation costs.

The RTU conditions the occupied space by forcing outdoor air mixed with return air from the space through the cooling and heating coils. The air mixture is comprised of at least 20% outside air and 80% return air from the conditioned space. In the event that the outside air is suitable for cooling, the minimum outdoor air intake may be increased up to 100%. Otherwise, cooling of the mixed airstream is done with either a direct expansion refrigeration cycle or chilled water supplied by the building chiller. Heating of the airstream is performed with a coil that heated water travels through, or the air is heated on contact with a gas-fired or electric burner. An illustration of the process is shown in Figure 3 [7].

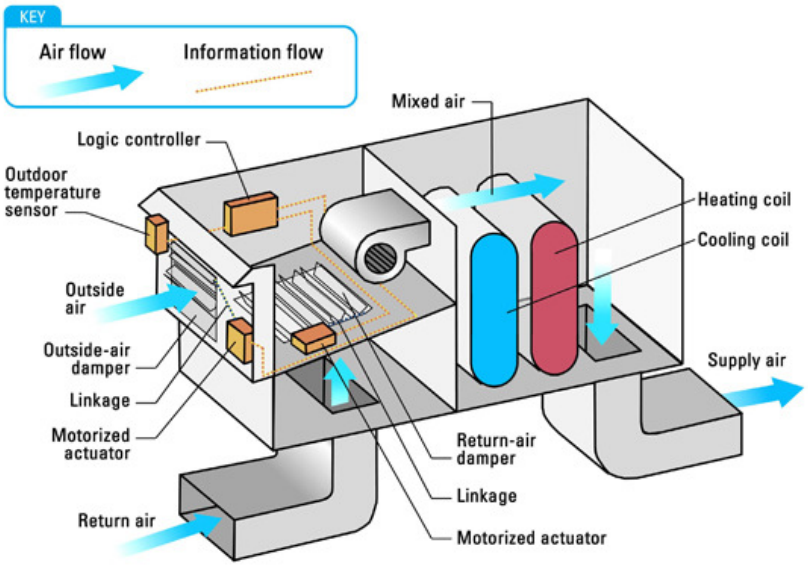

Figure 3 - Rooftop Unit Flow Diagram (Source: www.energystar.gov)

Control of airside HVAC equipment, including RTUs is regularly implemented with a system of single-input, single-output, PID loops. Each loop regulates a single process independently, whether it's airflow, discharge air temperature, or relative humidity, if applicable. The straight-forward and practical implementation of PID control makes it suitable for most applications. In fact, PID-based control is implemented in more than 90% of industrial and commercial controllers in use today [8].

1.3 PID Control

To understand how a PID process works, it is useful to diagram a control function. A block diagram of the familiar temperature feedback control process is shown in Figure 4.

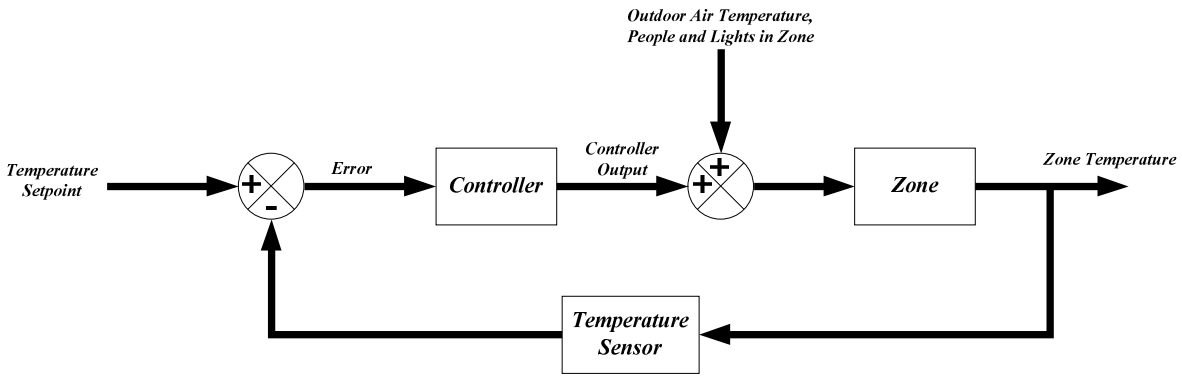

Figure 4 - Feedback Control System of a Zone Temperature Process

The general case of the single-loop control system is shown in Figure 5.

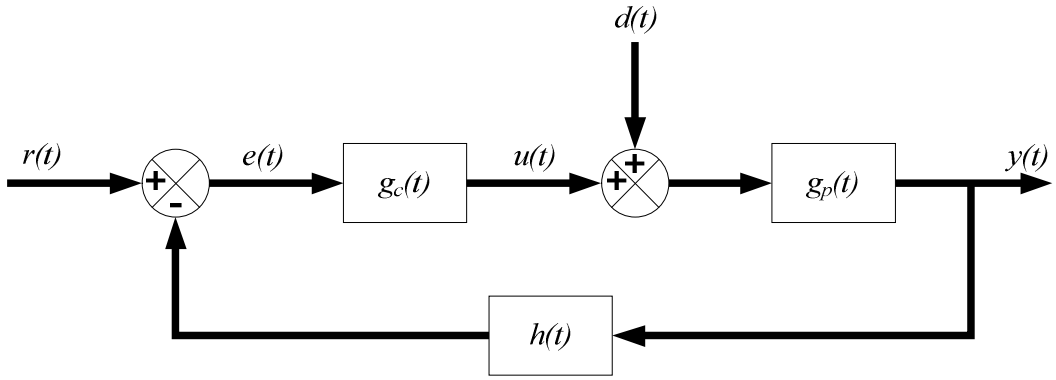

Figure 5 – Control System Expressed Formally in the Time-domain [9]

During the process, the controller, $g_c(t)$, produces an output, u(t), which depends on the difference between the current measurement reading, h(t), and the desired setpoint, r(t). At the next cycle, the sensor samples the output, y(t), and transmits an updated reading. The iterations occur continuously until the system reaches steady state, at which point the controller takes action to maintain the measured variable within a specified bound of setpoint. External perturbation signals, d(t), may act on the system and are accounted for during feedback.

The controller response to the error signal, e(t), is governed by its control law, which is determined to meet closed-loop performance specifications. The general case of the PID control law is formally expressed as [9]:

$$u(t) = k_p \cdot e(t) + k_i \cdot \int_0^t e(t) + k_d \cdot \frac{de(t)}{dt}$$

where k_p, k_i, and k_d represent the proportional, integral and derivative gains, respectively, thus the acronym, "PID".

The proportional term contributes to the controller response according to the difference between sampled output and the setpoint. The higher the k_p value, the faster the response of the system. A balance between a fast response time and oscillatory response must be reached with the proportional term. Also, proportional-only control does not guarantee zero steady-state error. Steady-state error is eliminated with the use of an integration term.

Generally, because HVAC processes are predominantly first-order, PI control algorithms are sufficient. The use of a derivative gain is beneficial for higher-order systems, representing faster dynamics. The reason for this is because the magnitude of the derivative term governs the controller response to the rate of change in the process variable. For example, consider the processes which are more

sensitive to control input, as in the case of a large control capacity relative to what's required to maintain the process variable at setpoint.

Reliable control of most HVAC systems can be achieved with linear, PID control. However, for a building composed of multiple, interacting subsystems with economic objectives, optimization of the entire plant in real-time is not possible with individual PID loops alone. Factors affecting control performance such as internal loads, weather, electricity pricing and plant dynamics are all predictable within a certain degree in real-time. This information can be used to calculate control moves sent to the plant to minimize cost while maintaining thermal comfort. A PID control scheme is incapable of processing internal building loads, weather data, electricity pricing and plant dynamics for computing predictions and control sequences around optimizing the plant in real-time.

1.4 Model Predictive Control

The time-varying conditions in the system present an opportunity for cost savings using a control method known as model predictive control (MPC). Model predictive control can be used to optimize the plant in real time by solving an objective function at each sampling instant throughout the course of the day. It differs from optimal control in that system constraints are dealt with in the control calculations. An on-board model of the plant is used in the controller to predict the plant behavior over the next *k* sampling intervals, or horizon. From this information, the set of *k* open-loop control sequences is computed. At the current time, t, the first open-loop control sequence is applied to the plant. State feedback of the plant captured at each sampling time is used to update model parameters and compute the next set of future control sequences, thereby operating in closed-loop. The cycle repeats in a receding horizon fashion. Figure 6 represents the workflow of the MPC algorithm, and Figure 7 illustrates plant control.

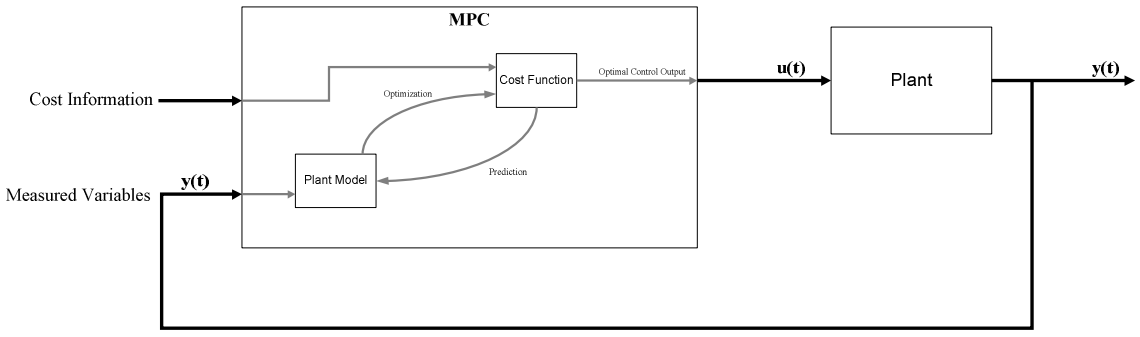

Figure 6 – Workflow of the Model Predictive Control Algorithm

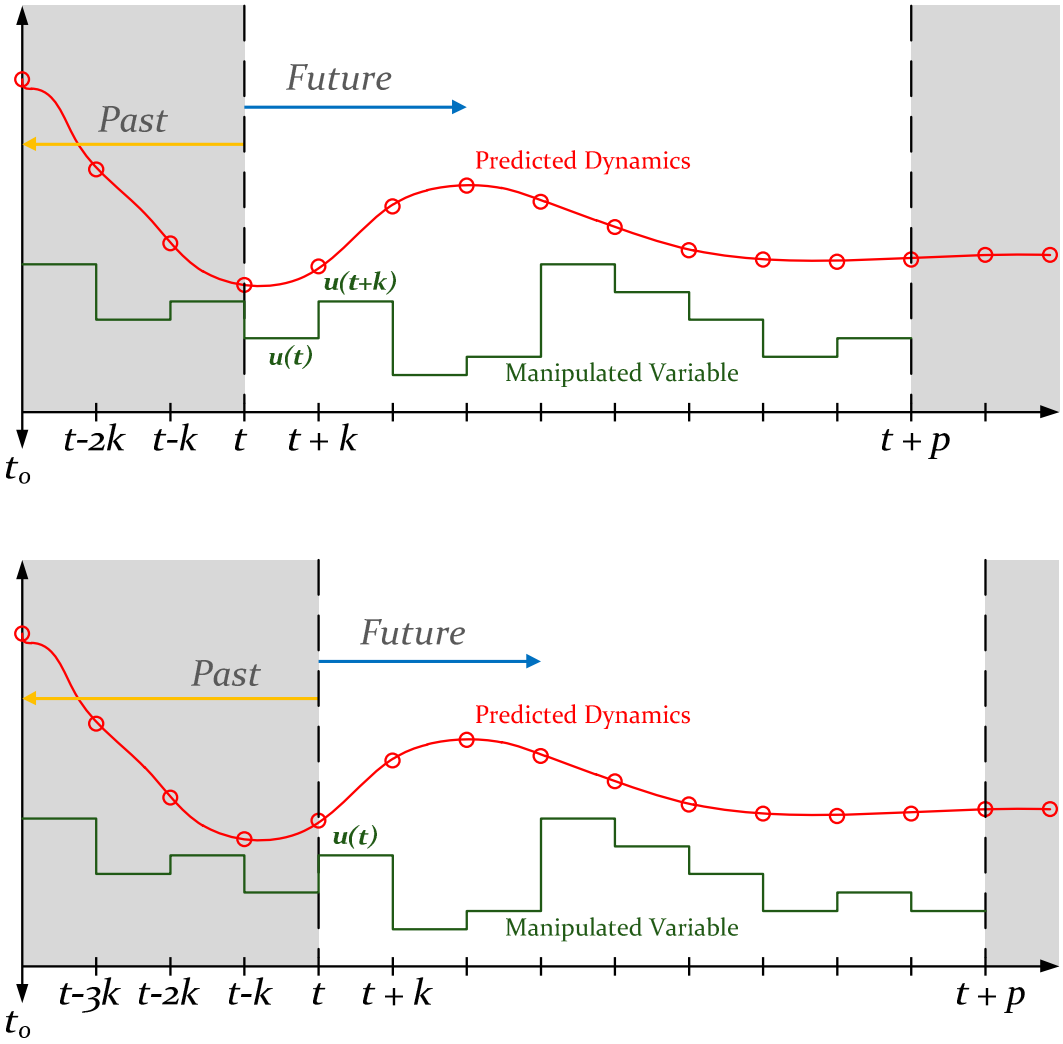

Figure 7 – Graphical Description of Model Predictive Control

The optimization of the plant occurs at each time step. The state feedback of the plant is used to compare the current state of the plant to the expected state of the plant given the last set of control outputs issued. The on-board model is reconciled so that more accurate predictions may be made in the future. The MPC must make trade-offs in control decisions, and the cost function contains such information. Depending on the goal of the plant, the cost function may be economic or quadratic. An economic function is a linear statement regarding the trade-offs in plant output versus resource expense. The aim of an economic objective is to directly maximize profit or minimize cost of plant operation, in real-time instead of tracking a setpoint [10]. If the objective is stated as quadratic, the control tracks a setpoint while minimizing deviation of the system state from the desired state. For instance, the manipulated variables are weighted according to their preference. The variables which are preferred to be maintained are weighted with higher cost for deviation from their setpoints. Variables which are less important are weighted with lower penalties for deviation. In other words, the objective function describes the preferences in making trade-offs in the plant variables. Additionally, constraints bound the set of manipulated variables which limit their minimum or maximum values or their minimum or maximum rate-of-change.

The experimentation with MPC in the HVAC space is nothing new [11]. Model predictive control algorithms have been proposed for the benefit of realizing energy savings subject to thermal comfort constraints [12], [13], [14], [15], [16], [17] and

[18]. However, in these works, real-time optimization of zone temperature in the presence of varying electricity pricing is not considered. Hence, cost savings and energy savings are not necessarily the same objectives [19, p. 7]. MPC algorithms for the purpose of demand response applications (incentivized peak load shifting) are presented in [20], [21] and [22]. Within these examples, model predictive control is proposed as centralized, de-centralized and distributed architectures.

In the centralized approach to MPC implementation, the entire plant model exists in one, central controller. The controller receives all the sensor inputs from the plant that are needed for it to run its routine. In this case, controller could refer to a desktop PC or centralized server. Although ideal, the centralized implementation is not a favorable choice for plants with multiple subsystems, as all the sensor information and optimization calculations for every subsystem would be processed in a single controller. Greater computational resources are required to execute the calculations in an effective, efficient manner. Because of this, destabilizing the system is a major concern. Another weakness is if the central controller ever stalled, the entire system would be dysfunctional. These reasons make the use of centralized MPC impractical for control of multiple, interacting systems.

The de-centralized architecture addresses the issue of multi-subsystem control by dividing up the control responsibility among dedicated controllers. Each of the individual controllers computes their optimal outputs autonomously and unaware

of the system states or control outputs in subsystems upstream or downstream from them. In other words, there is no communication exchange between controllers (often referred to as agents). Therefore, influences from nearby subsystems are considered as unknown disturbances. In fact, current PID algorithms operate in this way (without the model-based prediction, of course). The weakness in this arrangement, however, is in the case of a multi-zone system where the inter-zone influence is significant. A more collaborative approach to control of the system in which the agents share information with one another is beneficial for coping with the stronger couplings.

From a hardware perspective, there are indirect constraints on stability, namely computing power and controller communication. The complexity of the control system calculations and the increase of data traffic through the network pose challenges to system stability. Whether the plant is a series of chemical reactors or a collection of HVAC equipment, stability of the system is always a necessity. The selection of an appropriate control hierarchy in design of the control system addresses this concern. A few of the common architectures are described in the following sections. Each configuration is more fit than the others for certain applications.

Distributed MPC architectures enable state feedback of the plant to be shared among controllers and used in their control sequences. In this way, information

regarding subsystem interactions is taken into account in a method prescribed by the control systems designer. The advantage is that for each subsystem, the influences from neighboring subsystems are incorporated into the control objective. So there is opportunity to achieve better control performance than in the de-centralized configuration without requiring demanding plant-wide calculations at each sampling interval. This is especially true for tightly coupled subsystems in a plant.

Information exchange among controllers requires inter-controller networking. Unnecessary communication on the network adds traffic at marginal benefit to the control performance. Therefore, partially connected algorithms are implemented when information from any regulator is shared with a strict subset of the others. In this case, plant performance does not depend on complete communication between regulators. For example, subsystems with dedicated regulators only communicate with the regulators of subsystems which are directly coupled. Otherwise, a fully connected algorithm is implemented if it is deemed that full information exchange from one subsystem to all other subsystems in the plant is required. Such is the case if variables within subsystems have a strong influence on variables in neighboring subsystems.

Distributed agents operate collectively or independently in the control of the system. Collective control of a plant is implemented such that each agent minimizes

a global objective function. Conversely, regulators can be programmed to minimize a local performance measure independently of the others. The choice of either strategy requires the consideration of the communication requirements between agents at each time step. Information exchanged among agents only once within time steps will reduce traffic on the network, but control performance could be compromised. Distributed MPC agents control may either operate in a cooperative or non-cooperative fashion. One approach is that each of the local controllers minimizes a local objective function. It has been observed that a Nash equilibrium can be achieved, such that suboptimal performance is exhibited [14]. On the other hand, all the controllers communicate with a central coordinator in an effort to minimize one global cost function that considers the entire plant.

Over thirty distributed MPC strategies have been proposed in the literature for applications in hydro-electric dam control, chemical reactors and supply chains to name a few [23]. However, the published works relevant to the application of air-side HVAC systems are presented in Chapter 2 as a lead-in to formulating the problem addressed by this project.

1.5 Research Objective

Consider the two-zone space laid out in Figure 8. The space shown represents a single floor having an interior zone surrounded by an exterior zone, similar to an office building or retail space in which the floor is largely open, having little or no walls separating the individual air-side zones. A single rooftop unit in this case does not have sufficient capacity to condition the entire space, so the space is divided into two, discrete zones. The cooling load in each zone is met with a single, independent rooftop unit. Both units are controlled with a single field-device controller, which is part of the building automation network. This arrangement is not uncommon in practice.

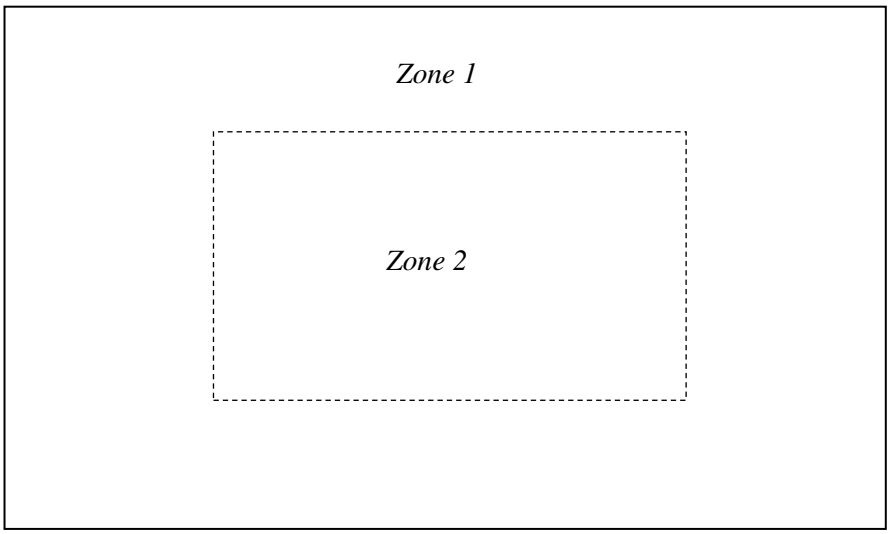

Figure 8 - Two-Zone System

The goal is to maintain the zone temperature within the prescribed thermal comfort bounds while minimizing cost over the 24-hour period. Both cost and thermal comfort are competing objectives which need to be managed, and therefore presents an opportunity for predictive, economic control in the presence of time-varying electricity pricing. Furthermore, each zone will experience different loading throughout the day, both internal loads developed from occupants, lights and computers and external loading due to weather conditions. The thermal mass of each zone, which determines its respective time constant for step inputs and has implications for control will need to be considered. Given that the sizes of both conditioned spaces differ, and thus the corresponding capacities of each rooftop unit, peak efficiency is attained at a different operating point for each unit. Additionally, the thermal influence of each zone on the other is significant and must be considered. The problem is one of a multi-variable, time-varying system in which economic trade-offs in variables can be made to achieve optimal performance. For this reason, a more advanced control system is required because PID control is incapable of calculating economic trade-offs while plant conditions vary over time.

A model-predictive control approach will be employed. Each zone MPC will be fed predictions for load profiles, electricity costs and weather data for the future horizon, and use these predictions in determining the optimal temperature setpoints each zone will control to for the objective of least monetary cost.

The calculation of the optimal temperature setpoint trajectories for both zones is burdensome for a single, building automation controller. Apart from maintaining plant stability, placing the computational burden in a single controller requires more computing horsepower, amounting to additional cost. By distributing the control responsibility among both controllers, the problem of computational hardware is addressed. Distributed control is appropriate because the existing building automation network controllers can be leveraged. The element of modularity introduced with distributed control also means that should parts of the plant be modified in the future, only those local controllers need to be changed. Whereas, single-sourcing the plant control function and model in one, central controller will require the entire plant model and control software to be modified.

Coverage in the literature of centralized and distributed MPC algorithms for the objective of minimizing energy consumption is established. Additionally, the development of centralized MPC algorithms for the purpose of demand response has been explored. Where the domain falls short is in the use of distributed MPC algorithms for demand response applications.

Thus, the novelty in this paper is the proposal of a distributed model-based, economic control strategy for cost savings in operating the building-wide HVAC air-side systems, in the presence of real-time electrical pricing. The control effort is divided among two controllers, each dedicated to its respective zone. Hence, the

computational load is divided into solving two smaller problems, and communication between the individual model-predictive controllers is enabled for improved performance over decentralized MPC. The solution allows a scalable network of controllers to communicate the necessary information needed for each controller to determine its optimal control action at a local level, while all collectively achieving the near-optimal control across the entire plant. Furthermore, the use of distributed MPC in the field can leverage the existing building automation network.

The proposed algorithm's effectiveness will be tested in simulation based on the criteria that utility bill cost savings is realized. The proposed distributed MPC strategy will be tested and compared with the performance attained with the centralized implementation as a benchmark. Then the results of the distributed MPC simulation will be compared to the decentralized MPC simulation. It is expected that performance of the distributed MPC, measured in cost, will improve over that of the decentralized MPC.

1.6 Organization of Thesis

Chapter 2 – In the following chapter, a brief history of MPC will be given. Examples presented in the literature pertaining to MPC for demand response applications will be reviewed. A more detailed review of distributed MPC algorithms applied to the HVAC space will be presented.

Chapter 3 – In chapter 3, the control problem is formulated. The theory for solving the control problem is developed, and the experimental tools and methodology employed in this research are visited. The simulation framework and test cases are presented in detail, and an analysis of the results is provided.

Chapter 4 – In this chapter, the conclusions drawn from the results are presented. Test cases in which exceptional results were observed are highlighted, and directions for future work are recommended.

Chapter 2: Literature Review

2.1 History of MPC

In its earlier stages of development, model predictive control was used by engineers at Shell Oil in the 1970s [24]. The technology was presented as Dynamic Matrix Control (DMC) by Cutler & Ramaker at the national AIChE Meeting in 1979. The DMC algorithm used an explicit plant model to predict future plant behavior over a finite prediction horizon. An unconstrained quadratic objective function was solved to compute the optimal state trajectory to track the given setpoint. Application to the temperature control of a furnace was tested. Published results showed the control performance of the DMC algorithm to be favorable compared to that of the benchmark PID lead/lag compensator. However, control of the process was unconstrained, which DMC in its original form was used for. Any constraint handling of a multi-variable process had to be done ad hoc. So the development of constrained control algorithms with DMC began to take shape.

MPC became more useful in the chemical processing and petroleum industries showing its value in reducing process costs and increasing process efficiency. Because of this value, applications of MPC in the HVAC space have received more research interest. Recent MPC development for use in HVAC system control shows promise in minimizing electricity costs, energy use or both.

2.2 MPC for Demand Response

Ma et. al. propose an economic model predictive control technique with the aim of reducing energy cost in a single-story commercial office building [21]. A model of the building is developed using EnergyPlus. The space is divided into five discrete zones. Each zone is served by a dedicated VAV terminal box which delivers the necessary cooling required to meet the load in the zone. In the simulations, weather data for Chicago, Illinois was used. Additional information about the building is described in Table 1. The layout is shown in Figure 9.

Floor area	5000 ft^2
Orientation	30° east of north
Window to wall ratio	0.29
Internal loads	
Occupant	1 occupant/100 ft^2
Lighting	16.18 W/ft^2
Equipment	10.79 W/ft^2
Occupied hours	7:00–18:00
Cooling system	VAV direct expansion (DX)
Heating system	N/A
Natural ventilation	N/A

Table 1 – Building model parameters for floor plan in Figure 9 [21]

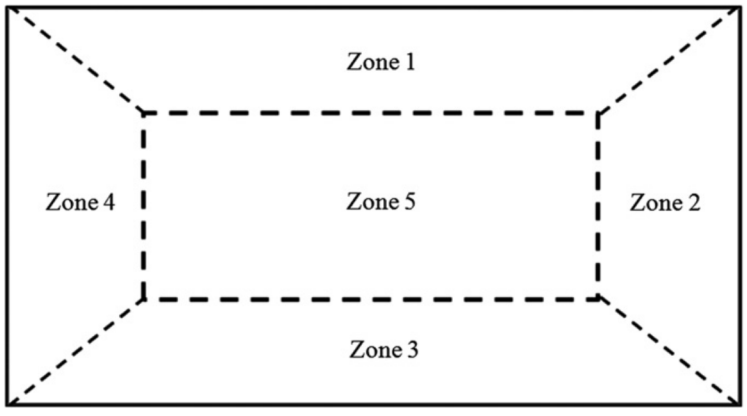

Figure 9 - Five zone office building layout [21]

A centralized approach is described which leverages a linear, economic objective function for optimally pre-cooling the building zones in the presence of time-varying utility pricing. The objective function is stated as:

$$\min \; J = C_e + C_d$$

where C_e represents the energy costs, and C_d represents the electrical demand cost.

$$C_e = \sum_{t=1}^{N} [Ec(t) \cdot \Delta t \cdot P(t)]$$

$$C_d = Dc \cdot \max_{t_d \leq t \leq N} \{P(t)\}$$

P(t) and Ec(t) are the power use and electrical charge rate, respectively, at the current time, t. Dc denotes the demand cost, and N denotes the time steps per day. The value of Δt is equal to 0.25 hours, meaning the electrical charge rate is updated every 15 minutes per the rate plan described by TOU-GS-3 from Southern California Edison (SCE). A detailed break-down of the energy costs are shown in table 2.

	Energy charge ($ / kWh)	
Summer season Jun. 1–Oct. 1	On-peak 12:00–18:00 weekdays except holidays	0.31176
	Mid-peak 8:00–12:00, 18:00–23:00 weekdays except holidays	0.14200
	Off-peak 23:00–08:00, weekdays and all day on weekends and holidays	0.06866
Winter season Oct. 1–Jun. 1	Mid-peak 8:00–21:00 weekdays except holidays	0.10468
	Off-peak 21:00–8:00, weekdays and all day on weekends and holidays	0.07151

Table 2 - Energy Charge Rate for TOU-GS-3 [21]

The problem is solved with the linear programming routine in Matlab. The demand cost term is converted to a linear term for this purpose. At the current time, k, the energy cost, $C_e(k)$ is decomposed into two terms:

$$C_e(k) = C_{e,h}(k) + C_{e,f}(k)$$

$C_{e,h}(k)$ represents the energy cost before k, and $C_{e,f}(k)$ represents the predicted energy cost in the future horizon.

$$C_{e,h}(k) = \sum_{t=1}^{k} [Ec(t) \cdot \Delta t \cdot P(t)]$$

$$C_{e,f}(k) = \sum_{t=k+1}^{N} [Ec(t) \cdot \Delta t \cdot P(t)]$$

The variable, z, is introduced to represent the peak demand during the day.

$$z = \max_{t_d \le t \le N} \{P(t)\}$$

and y(k) is defined as:

$$y(k) = [P(k+1) \quad \cdots \quad P(k+N_p)]^T$$

$N_p = N - k$ is the width of the prediction window, which extends from the current time until the last time step of the day. In this scheme, the prediction window shrinks as the day draws on. This contrasts with the more familiar MPC scheme where the window slides through the day, having a fixed width.

The objective function is simplified as follows, and the costs are optimized over the course of a day.

$$\min \tilde{J}(k) = C_{e,f}(k) + C_d = \begin{bmatrix} Dc & Ec_f^T(k) \end{bmatrix} \begin{bmatrix} z \\ y(k) \end{bmatrix}$$

z is incorporated into the optimization problem:

$$z \geq \max_{t_d \leq t \leq k} \{P(t)\}$$

$$\begin{bmatrix} -1 & 1 & 0 & 0 & 0 \\ -1 & 0 & 1 & 0 & 0 \\ \vdots & 0 & 0 & \ddots & 0 \\ -1 & 0 & 0 & 0 & 1 \end{bmatrix} \begin{bmatrix} z \\ y(k) \end{bmatrix} \leq \mathbf{0}$$

x(k) and U(k) are set as augmented vectors of zone temperature and temperature setpoints over the control horizon, N_c, respectively:

$$x(k) = \begin{bmatrix} T_z^T(k+1) & \cdots & T_z^T(k+N_c) \end{bmatrix}^T$$

$$U(k) = \begin{bmatrix} T_{sp}^T(k) & \cdots & T_{sp}^T(k+N_c-1) \end{bmatrix}^T$$

and N_c is selected to be equal to N_p.

Additional inequality constraints are imposed to regulate the zone tmperature and setpoints within a bound range.

$$T_{sp,min}(k) \leq U(k) \leq T_{sp,min}(k)$$

$$T_{z,min}(k) \leq x(k) \leq T_{z,max}(k)$$

Thus the objective function can be written in linear form as:

$$\min_{\Psi} \tilde{J}(k) = \begin{bmatrix} Dc & Ec_f^T(k) & \mathbf{0} & \mathbf{0} \end{bmatrix} \begin{bmatrix} z \\ y(k) \\ x(k) \\ U(k) \end{bmatrix}$$

where $\Psi = [z \quad y(k) \quad x(k) \quad U(k)]^T$ is the decision vector.

At each time step, only the first element of U(k) is sent to the model, and the optimization problem is solved at each subsequent time step.

The algorithm was tested on the model in which a seven-day period was simulated. Compared to the baseline case, the results exhibited that the demand response MPC had a cost savings of 28.52% versus the 17.42% savings achieved with a linear-up strategy. The step-up strategy showed to have 24.35% cost savings. In the step-up and linear-up strategies, the zone temperature is allowed to remain at the lower bound of the comfort region until the on-peak charge rate begins, at which point the setpoints are raised in a linear, or step-up fashion. The study does not investigate the possibility that the zones have an unequal amount of thermal mass.

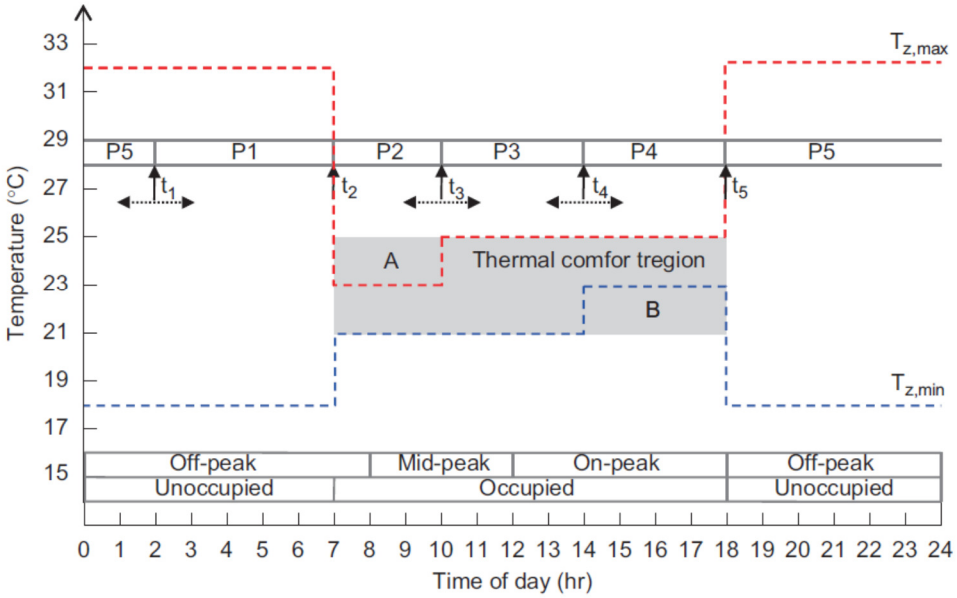

Figure 10 - Zone setpoints step-up throughout the day [21]

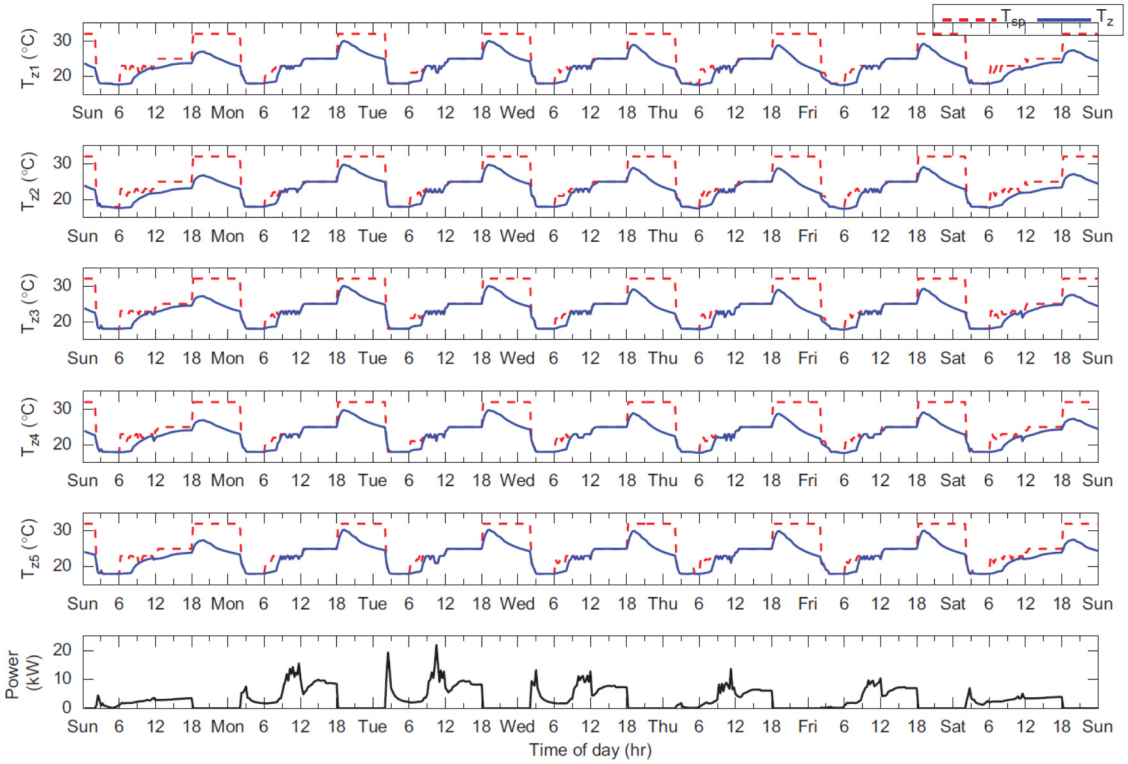

Figure 11 - Zone temperature setpoints and power profile of simulated 7-day period [21]

Model predictive control for the use of minimizing peak power consumption of an electric cooling system for a commercial building located in Jeju Is., Korea is proposed [22]. A linear, economic objective function is presented for determining the optimal power required to maintain a single zone space between 26°C and 28°C.

$$J = \sum_{k=1}^{N} \{u(k) \cdot p \cdot c(k)\} + p_{max} \cdot C_{cp}$$

$$\text{s.t. } T_{low} \leq T_t \leq T_{high}$$

The TOU pricing and the critical peak price are the weights in the objective function. The cost information is presented in Figure 12 and Table 3.

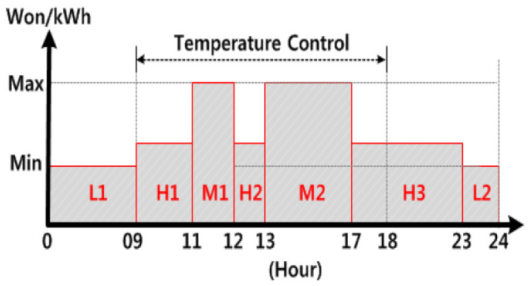

Figure 12 – Typical summertime electrical rates [22]

Period	Cost
off-peak (L1, L2)	52.6[won/kW]
mid-peak (H1, H2, H3)	100.4[won/kW]
on-peak (M1, M2)	172.9[won/kW]
CP charge (C_{cp})	350.0[won/kW]

Table 3 – Electrical rates shown in Figure 12 [22]

The building parameters are detailed in Table 4.

Parameters	Value
Volume zone	253[m^3]
Ventilation	1[h]
Façade surface	49[m^2]
Façade heat resistance	0.11[m^2K/W]
Floor and internal walls surface	122[m^2]
Window surface	44[m^2]
Window heat resistance	3.6[m^3K/W]

Table 4 – Parameters of building model [22]

Comparison of the results generated by the proposed algorithm is made against the performance of an on/off type control system.

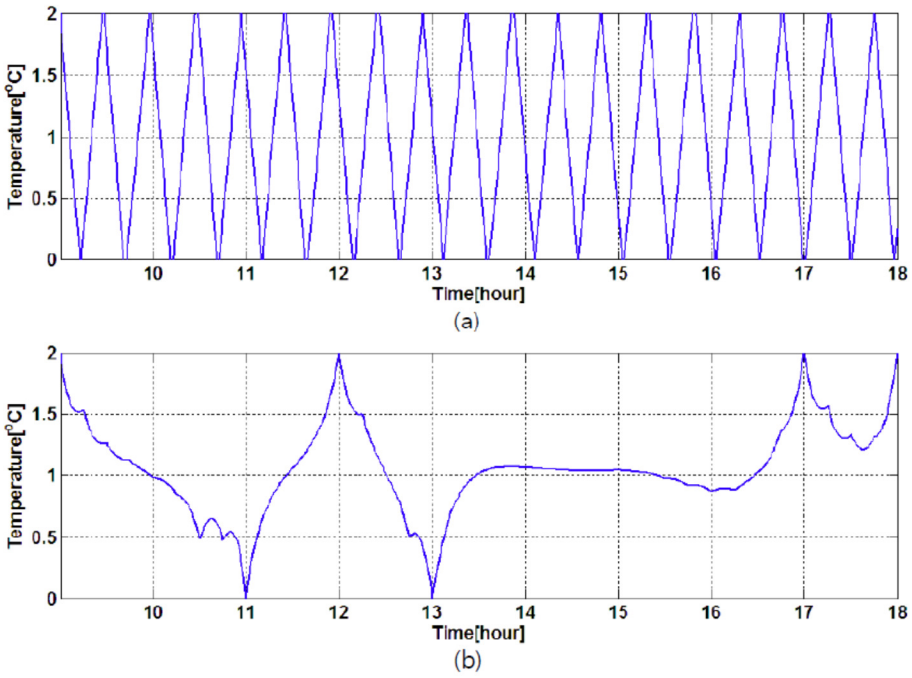

Figure 13 – Comparison of internal temperature for (a) on/off control and (b) MPC with linear programming. 0°C indicates 26°C, and 2°C indicates 28°C. [22]

The single-zone MPC method exhibited a TOU savings of 4.57% and a CP savings of 42.85% per day. About 1.6 kW is used during the peak hours with the MPC scheme versus 2.8 kW with the on/off only control. A comparison to a PI-type control scheme is not given. The approach presented pertains to a commercial setting; however, it does not consider control of multiple zones and their interactions.

In the preceding examples, thermal comfort is dealt with by imposing fixed constraints on the range of temperature setpoints issued by the MPC. However, incorporating a thermal comfort preference into the cost optimization problem is proposed in [20]. Temperature setpoints are assigned to price ranges according to the occupants' discomfort-tolerance index. Consequentially, a control policy is developed which aims to reduce the user's electrical costs while maintaining comfort based on the user's preferences.

The cost function and constraints is proposed [20]:

$$\min_{u[\cdot],T_r[\cdot]} = \sum_{t=1}^{N}(q * l[t] * u[t])^2 + \sum_{t=1}^{N}(w * (T[t] - T_r[t]))^2$$

$$\begin{aligned} & u[t] \in [0,1] \quad \forall t \{1..N\} \\ s.t.\ & T(t) = G(u[t], x(t)) \\ & T[t], T_r[t] \in [T_{\min}, T_{\max}] \quad \forall t \in \{1..N\} \end{aligned}$$

The cost function describes the trade-off between energy consumption (first term) and thermal comfort (second term), where the variables, q and w, are weights according to preference. The higher the value of one weight relative to the other, so is its priority in the objective. The aim of the MPC is to minimize the sum of the terms by sending the optimal signals, u(t), to the AC system.

It is proposed that the preference in thermal comfort is handled with a temperature setpoint assignment algorithm, such that temperature setpoints are assigned to price ranges over the course of the day. It is assumed that the daily prices at each hour are known one day in advance as is the case with day-ahead pricing. The determination of which temperature setpoints are assigned to the price ranges is done with a discomfort tolerance index, α. A value of $\alpha > 0$ means the user has a higher tolerance for discomfort, and higher temperature setpoints are assigned to wider price ranges. A value of $\alpha < 0$ means that the user has a lower tolerance for discomfort, and the higher temperature setpoints are assigned only to the highest price ranges. A neutral value of $\alpha = 0$ is to state that the user does not have any preference, and therefore the temperature setpoints are distributed evenly across all price ranges.

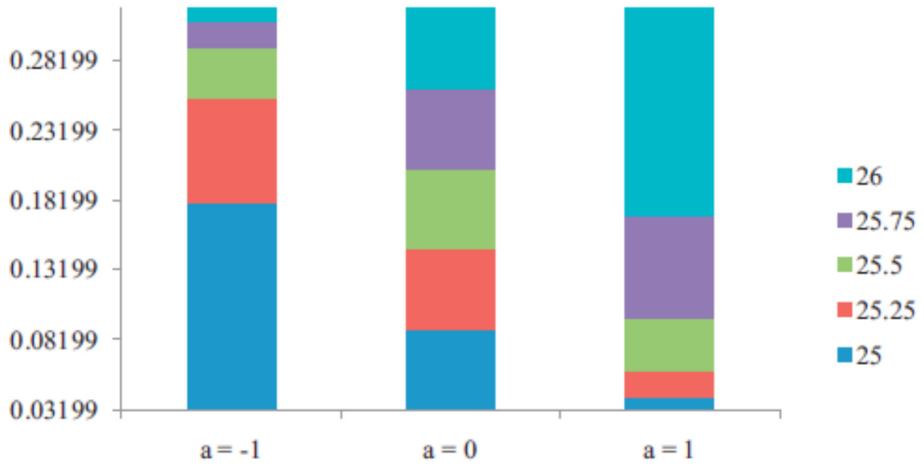

Figure 14 - Zone temperature setopints assigned to price ranges [20]

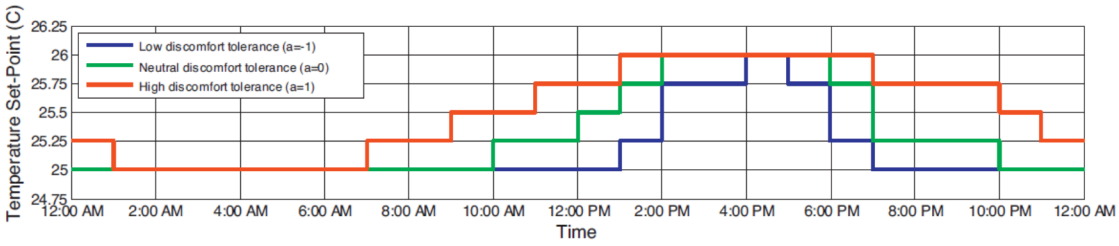

Figure 15 - Temperature setpoint assignment over 24-hour period [20]

It was found that using MPC alone resulted in a 13% reduction in cost over the standard two-position control scheme used in traditional practice; while the temperature setpoint assignment algorithm when paired with the MPC resulted in a 17.5% cost savings over the two-position control.

2.3 Distributed MPC

A distributed algorithm is proposed and tested for a two-zone building [25]. The zones are thermally coupled, and the coupling is modeled by the difference in temperature multiplied by a coupling constant.

$$q_1 = \alpha(T_2 - T_1)$$

$$q_2 = \alpha(T_1 - T_2)$$

Q and T represent the heat transfer and zone temperature of the zones, respectively. Alpha is the coupling constant; the higher value signifies a greater degree of thermal coupling between the zones.

Morosan et. al propose a distributed MPC strategy for temperature control of a three-zone system [16]. Each zone temperature is maintained with the input of a 1200-watt electrical convector heating unit. A double-glazed window of 2 m^2 is positioned within the larger external wall of each zone. The external walls are constructed of 1-cm of gypsum, 8-cm of extruded polystyrene insulation and 20-cm of concrete. The zones are partitioned with 7.2-cm thick gypsum board. The layout of the three-zone system is presented in Figure 16.

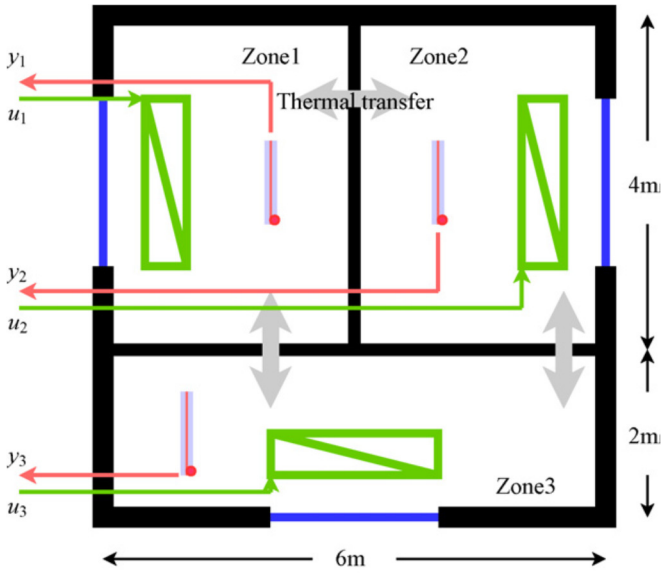

Figure 16 - Three-zone conditioned space [16]

The centralized problem is formulated and presented first as a performance benchmark for the distributed control strategy. The thermal model of each zone is individually represented in state space form as:

$$\begin{cases} \boldsymbol{x}_i(k+1) = \boldsymbol{A}_i\boldsymbol{x}_i(k) + \boldsymbol{B}_i \begin{bmatrix} u_i(k) \\ \boldsymbol{y}_{h_i}(k) \end{bmatrix} \\ \boldsymbol{y}_i(k) = \boldsymbol{C}_i\boldsymbol{x}_i(k) \end{cases}, i = 1 \dots 3$$

where $\boldsymbol{y}_{h_i}$ includes the outputs of all adjacent rooms which act on the local zone.

Therefore, the global model representing the dynamics of the three zones collectively, can be constructed as:

$$\boldsymbol{A}_g = \begin{bmatrix} \boldsymbol{A}_1 & \boldsymbol{B}_{12}\boldsymbol{C}_2 & \boldsymbol{B}_{13}\boldsymbol{C}_3 \\ \boldsymbol{B}_{22}\boldsymbol{C}_1 & \boldsymbol{A}_2 & \boldsymbol{B}_{23}\boldsymbol{C}_3 \\ \boldsymbol{B}_{32}\boldsymbol{C}_1 & \boldsymbol{B}_{33}\boldsymbol{C}_2 & \boldsymbol{A}_3 \end{bmatrix}$$

$$\boldsymbol{B}_g = \begin{bmatrix} \boldsymbol{B}_{11} & 0 & 0 \\ 0 & \boldsymbol{B}_{21} & 0 \\ 0 & 0 & \boldsymbol{B}_{31} \end{bmatrix}$$

$$\boldsymbol{C}_g = \begin{bmatrix} \boldsymbol{C}_1 & 0 & 0 \\ 0 & \boldsymbol{C}_2 & 0 \\ 0 & 0 & \boldsymbol{C}_3 \end{bmatrix}$$

$$\begin{cases} \boldsymbol{x}(k+1) = \boldsymbol{A}_g \boldsymbol{x}(k) + \boldsymbol{B}_g \boldsymbol{u}(k) \\ \boldsymbol{y}(k) = \boldsymbol{C}_g \boldsymbol{x}(k) \end{cases}$$

$$\boldsymbol{x}(k) = [\boldsymbol{x}_1^T(k) \quad \boldsymbol{x}_2^T(k) \quad \boldsymbol{x}_3^T(k)]^T$$

$$\boldsymbol{u}(k) = [\boldsymbol{u}_1^T(k) \quad \boldsymbol{u}_2^T(k) \quad \boldsymbol{u}_3^T(k)]^T$$

$$\boldsymbol{y}(k) = [\boldsymbol{y}_1^T(k) \quad \boldsymbol{y}_2^T(k) \quad \boldsymbol{y}_3^T(k)]^T$$

The control problem is stated as minimizing the global cost function, subject to the plant dynamics. The trade-off between energy use and thermal comfort are weighted in each of the three zones while taking into consideration the future occupancy profile. The global cost function is expressed in terms of the predicted output of each zone and the control output to each convector unit.

$$J(k) = \sum_{i=1}^{3} J_i(k)$$

$$J_i(k) = \sum_{j=N_1}^{N_2} \delta_i^k(j)|\hat{y}_i(k+j|k) - w_i(k+j)| + \lambda_i \sum_{j=0}^{N_2-N_1} u_i(k+j)$$

where N_1 and N_2 are the lower and upper bounds of the prediction horizon, respectively; $\hat{y}_i(k+j|k)$ is the predicted output, $w_i(k+j)$ represents the future reference, δ is the future occupation profile as the error weighting term, and λ is a coefficient that weights the control command.

$$\delta^k(j) = \begin{cases} 1, & k+j \in Occupied \\ 0, & k+j \in Unoccupied \end{cases}$$

The command weighting coefficient, λ, influences the steady-state error. A large value of λ is interpreted as energy being relatively expensive compared to maintaining comfort, and as a result reduced thermal comfort will be observed in the zone.

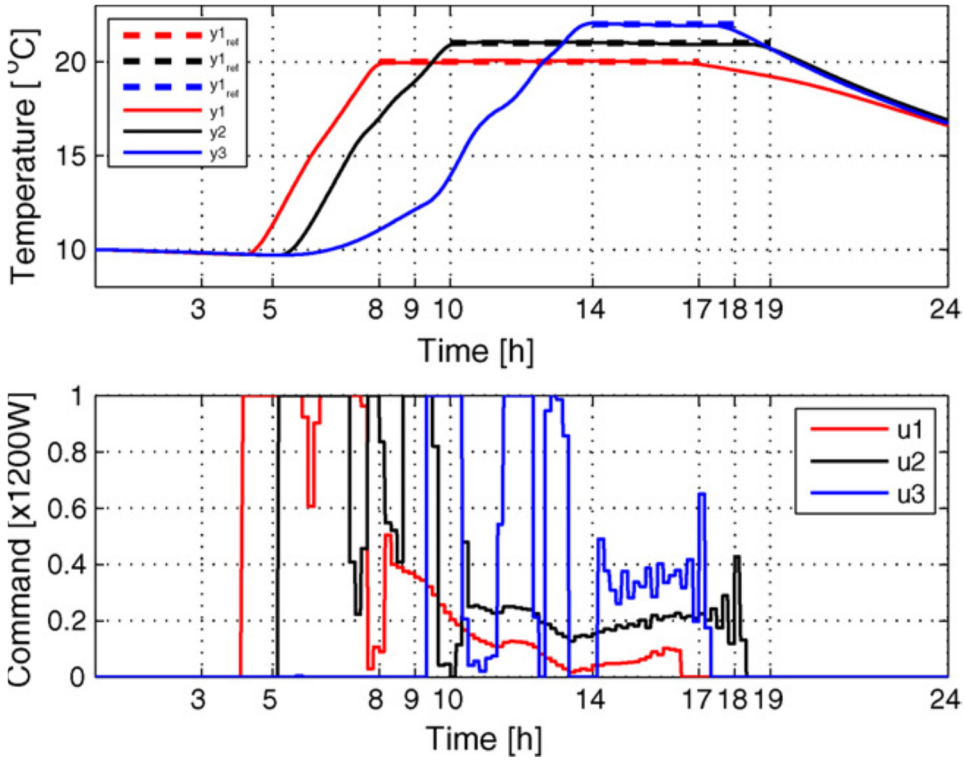

Figure 17 - Centralized MPC Simulation Results [16]

Simulation results for the centralized MPC showed no overshoot in the temperature, and all three temperatures were maintained without any noticeable deviation from their respective setpoints.

The distributed control problem is formulated by using the future predicted outputs of the neighboring rooms in the system.

$$\hat{\boldsymbol{y}}_i(k) = \boldsymbol{\Psi}_i \boldsymbol{x}_i(k) + \boldsymbol{\Phi}_{\mathrm{i1}} \mathbf{u}_{\mathrm{i}}(\mathrm{k}) + \sum_{\mathrm{s}\epsilon \mathrm{h_i}} \boldsymbol{\Phi}_{\mathrm{is}} \mathbf{y}_{\mathrm{s}}(\mathrm{k})$$

where

$$\hat{\boldsymbol{y}}_i(k) = [\hat{y}_i(k+N_1|k) \quad \cdots \quad \hat{y}_i(k+N_2|k)]^T$$

$$\boldsymbol{u}_i(k) = [u_i(k|k) \quad \cdots \quad u_i(k+N_u-1|k)]^T$$

$$\boldsymbol{\Psi}_{\mathrm{i}} = \left[\mathbf{C}_{\mathrm{i}}\mathbf{A}_{\mathrm{i}}^{\mathrm{N_1}} \quad \cdots \quad \mathbf{C}_{\mathrm{i}}\mathbf{A}_{\mathrm{i}}^{\mathrm{N_2}}\right]^{\mathrm{T}}$$

$$\boldsymbol{\Phi}_{\mathrm{i1}} = \begin{bmatrix} \phi_{\mathrm{i1}}^{\mathrm{N_1-1}} & \cdots & \phi_{\mathrm{i1}}^{0} & 0 & \cdots \\ \vdots & \cdots & \vdots & \ddots & \vdots \\ \phi_{\mathrm{i1}}^{\mathrm{N_2-1}} & \cdots & \cdots & \phi_{\mathrm{i1}}^{\mathrm{N_2-N_u+1}} & \sum_{\mathrm{k=0}}^{\mathrm{N_2-N_u}} \phi_{\mathrm{i1}}^{\mathrm{k}} \end{bmatrix}$$

$$\boldsymbol{\Phi}_{\mathrm{is}} = \begin{bmatrix} \phi_{\mathrm{is}}^{\mathrm{N_1-1}} & \cdots & \phi_{\mathrm{is}}^{0} & 0 & \cdots & 0 \\ \vdots & \cdots & \vdots & \vdots & \ddots & \vdots \\ \phi_{\mathrm{is}}^{\mathrm{N_2-1}} & \cdots & \phi_{\mathrm{is}}^{\mathrm{N_2-N_1}} & \phi_{\mathrm{is}}^{\mathrm{N_2-N_1-1}} & \cdots & \phi_{\mathrm{is}}^{0} \end{bmatrix}$$

$$\phi_{ij}^{k} = \boldsymbol{C}_i \boldsymbol{A}_i^k \boldsymbol{B}_{ij}$$

$$\boldsymbol{y}_s(k) = \begin{bmatrix} y_s(k) \\ \hat{y}_s(k+N_1|k-1) \\ \vdots \\ \hat{y}_s(k+N_2-1|k-1) \end{bmatrix}$$

The local cost function of each controller is expressed as:

$$J_i(k) = \delta_i^k \left| \boldsymbol{\Psi}_i \boldsymbol{x}_i(k) + \boldsymbol{\Phi}_{\mathrm{i1}} \mathbf{u}_{\mathrm{i}}(\mathrm{k}) + \sum_{s \epsilon h_i} \boldsymbol{\Phi}_{is} \boldsymbol{y}_s(k) - \boldsymbol{w}_i(k) \right| + \lambda_i \boldsymbol{e} \boldsymbol{u}_i(k)$$

where

$$\delta_i^k = [\delta_i^k(1) \quad \cdots \quad \delta_i^k(N_2 - N_1 + 1)]$$

$$\boldsymbol{e} = [1 \quad \cdots \quad 1] \epsilon \mathbb{R}^{N_2 - N_1 + 1}$$

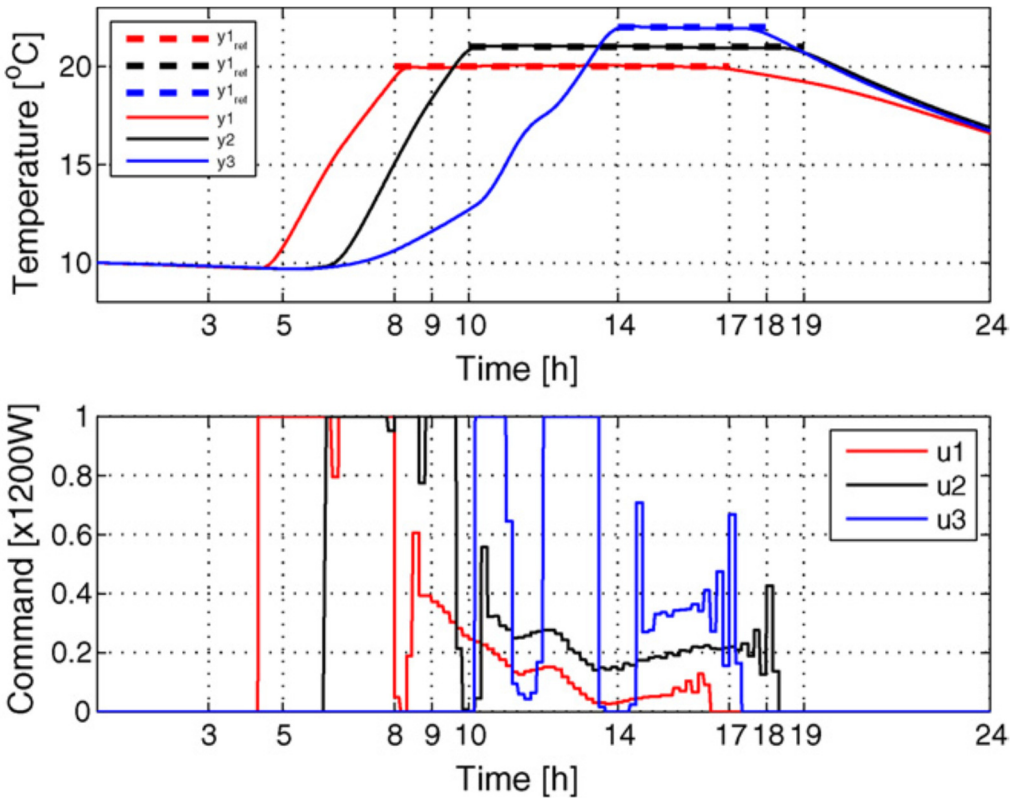

Figure 18 - Simulation results from the distributed MPC algorithm [16]

The control performance with the distributed approach agreed with that of the centralized approach. Thermal comfort was not sacrificed with the distributed strategy, and the power consumption for the 24-hour period was improved. The centralized strategy resulted in power consumption of 279 kW-h, and the power consumption of the distributed strategy was 273 kW-h. In this study the investigation of performance with combinations of different heat sources was not considered. Various degrees of thermal coupling amongst zones were not tested against the distributed MPC architecture proposed.

A distributed MPC approach based on Bender's decomposition is proposed for the purpose of minimizing energy bill costs when the conditioned space is served by multiple heating sources [26]. In this hierarchical approach, the plant-wide optimization problem is setup by defining a master problem to be solved at a central coordinator, and a sub-problem solved at each local controller.

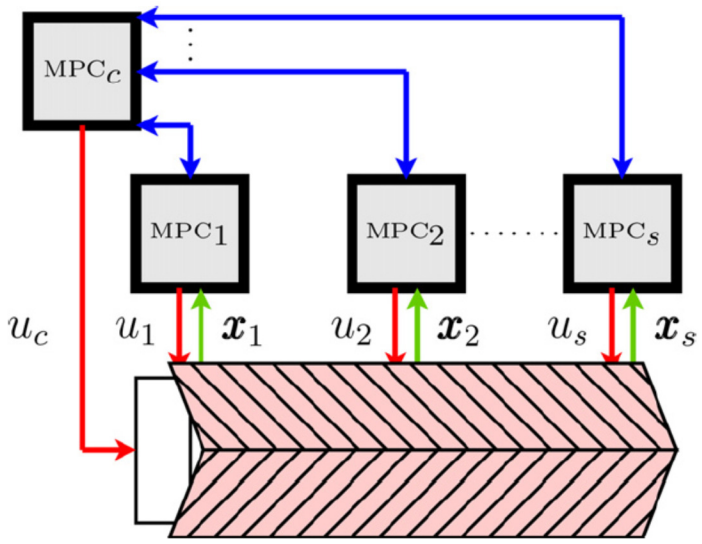

Figure 19 - Distributed MPC layout [26]

In this case, the MPC controllers provided outputs that served to actuate the heating capacity directly. Simulations were run on a three-zone building model. Each zone was modeled as being heated by a dedicated electrical convector unit (1200 W maximum power) and a single, central heating system. The energy use of the central heating system assumed a natural gas boiler with a specified efficiency, water density and water mass flow rate. The three-zone model was simulated using

the Matlab toolbox, SIMBAD. Each room is assumed to have a double-glazed window of 2m2 area on the surface of the exterior wall. The exterior wall is constructed of 1 cm gypsum, 8 cm of extruded polystyrene and 20 cm of concrete. The internal wall dividing the zones is 7.2 cm thick and is made of gypsum board. It is assumed that the air in the space is perfectly-mixed.

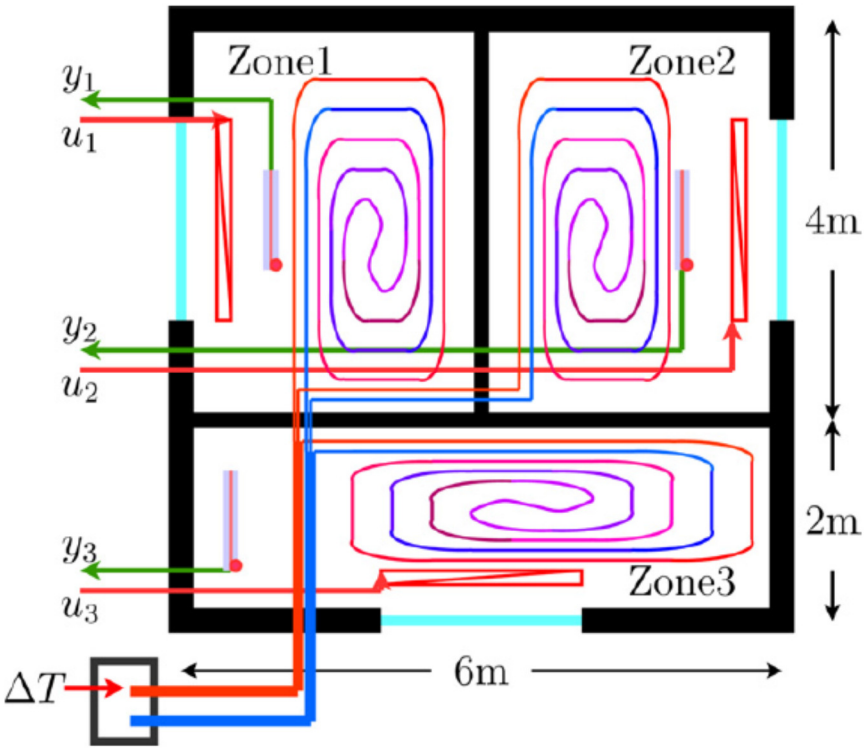

Figure 20 - Three-zone floor-plan of simulated building [26]

Given the linear, discrete-time state space representation of a zone, i:

$$\begin{cases} \boldsymbol{x}_i(k+1) = \boldsymbol{A}_i \boldsymbol{x}_i(k) + \boldsymbol{B}_{ic} u_c(k) + \sum_{j \in \hbar_i \cup \{i\}} \boldsymbol{B}_{ij} u_j(k) \\ y_i(k) = \boldsymbol{C}_i \boldsymbol{x}_i(k), \end{cases} \quad \forall i \in S,$$

where $\boldsymbol{x}_i \in \mathbb{R}^{n_i}, \ \forall i \in S$ is the local state, and $u_i, u_c, y_i \in \mathbb{R}, \forall i \in S$ are the local electrical power input, shared boiler power input and the measured zone temperature, respectively.

The prediction equation is written as:

$$\begin{aligned} \hat{\boldsymbol{y}}_i(k) &= [\hat{y}_i(k+1|k) \quad \cdots \quad \hat{y}_i(k+N_2|k)]^T \\ &= \boldsymbol{\Psi}_i \boldsymbol{x}_i(k) + \boldsymbol{\Phi}_{ic} \boldsymbol{u}_c(k) + \sum_{j \in \hbar_i \cup \{i\}} \boldsymbol{\Phi}_{ij} \boldsymbol{u}_j(k), \end{aligned}$$

where $\boldsymbol{u}_i(k) = [u_i(k) \cdots u_i(k+N_u-1)]^T, \forall i \in S, \boldsymbol{u}_c(k) = [u_c(k) \cdots u_c(k+N_u-1)]^T$, and the control inputs outside of the horizon, N_u, are considered constant.

$$\boldsymbol{\Psi}_i = [(\mathbf{C}_i \mathbf{A}_i^1)^T \quad \cdots \quad (\mathbf{C}_i \mathbf{A}_i^{N_2})^T]^T,$$

$$\boldsymbol{\Phi}_{ij} = \begin{bmatrix} \phi_{ij}^0 & 0 & \cdots & 0 \\ \phi_{ij}^1 & \phi_{ij}^0 & 0 & \cdots \\ \vdots & \cdots & \ddots & \vdots \\ \phi_{ij}^{N_2-1} & \cdots & \phi_{ij}^{N_2-N_u+1} & \sum_{k=0}^{N_2-\bar{N}_u} \phi_{ij}^k \end{bmatrix}, \quad \forall j \in S \cup \{c\},$$

$$\phi_{ij}^k = \mathbf{C}_i \mathbf{A}_i^k \mathbf{B}_{ij},$$

$$\boldsymbol{c}_i'^T = [\, \boldsymbol{c}_i^T \quad \mathbf{0}_{1,N_u} \quad \mathbf{0}_{1,N_2} \quad \mathbf{0}_{1,N_2} \quad \lambda_i \mathbf{1}_{1,N_2} \quad \lambda_i \mathbf{1}_{1,N_2} \,],$$

$$\boldsymbol{c}_c'^T = [\boldsymbol{c}_c^T \quad \mathbf{0}_{1,N_u}], \qquad \boldsymbol{D} = [\boldsymbol{I}_{N_u,N_u} \quad \boldsymbol{I}_{N_u,N_u}], \qquad \boldsymbol{g} = \bar{u}\bar{u}_c \mathbf{1}_{N_u,1},$$

The objective is to minimize the energy cost of heating the building while maintaining thermal comfort. The thermal comfort region is bounded by an upper and lower temperature bound and is active only during occupied periods. The future occupation profile over the prediction horizon for room *i*, at time step *k*, is denoted as, $\delta_i(k) = [\delta_i(k+1) \cdots \delta_i(k+N_2)]^T$.

Each element of the occupancy vector is defined as:

$$\delta_i(k+j) = \begin{cases} 1, & k+j \in \text{occupation}_i \\ 0, & k+j \in \text{inoccupation}_i. \end{cases}$$

The optimization problem is stated as:

$$\min_{\boldsymbol{u}_c(k),\boldsymbol{u}_i(k),\forall i \in S} J(k) = \sum_{i \in S} \left(\boldsymbol{c}_i^T(k)\boldsymbol{u}_i(k) + \sum_{j=1}^{N_2} f_i(k+j) \right) + \boldsymbol{c}_c^T(k)\boldsymbol{u}_c(k),$$

subject to:

$$\mathbf{0} \le \boldsymbol{u}_i(k) \le \bar{\boldsymbol{u}}_i, \quad \forall i \in S,$$

$$\mathbf{0} \le \boldsymbol{u}_c(k) \le \bar{\boldsymbol{u}}_c,$$

The comfort penalty function is defined as:

$$f_i(k+j) = \begin{cases} 0, & \text{if } \overline{\mu}_i(k+j) \le 0 \text{ and } \underline{\mu}_i(k+j) \le 0 \\ \lambda_i \overline{\mu}_i(k+j), & \text{if } \overline{\mu}_i(k+j) > 0 \\ \lambda_i \underline{\mu}_i(k+j), & \text{if } \underline{\mu}_i(k+j) > 0, \end{cases}$$

with,

$$\underline{\mu}_i(k+j) = \delta_i(k+j)(\underline{w}_i(k+j) - \hat{y}_i(k+j|k)),$$
$$\overline{\mu}_i(k+j) = \delta_i(k+j)(\hat{y}_i(k+j|k) - \overline{w}_i(k+j)), \quad \forall i \in S, \ \ \forall j = 1, \ldots, N_2,$$

$$\boldsymbol{c}_i(k) = \left[c_i(k) \cdots c_i(k+N_u-2) \sum_{j=N_u-1}^{N_2-1} c_i(k+j) \right]^T,$$
$$\boldsymbol{c}_c(k) = \left[c_c(k) \cdots c_c(k+N_u-2) \sum_{j=N_u-1}^{N_2-1} c_c(k+j) \right]^T,$$

where $c_i(k+j)$ and $c_c(k+j)$ are the energy costs for the local electrical and shared boiler inputs, respectively at time step k+j.

The algorithm which solves for the optimal power input trajectory over the control horizon, while considering the thermal coupling among the three zones is stated [26]:

Require: Global problem (5), $\epsilon, \epsilon', \boldsymbol{x}_i, \ \ \forall i \in S$
Ensure: Control inputs $\boldsymbol{u}_c^{\prime *}, \boldsymbol{u}_i^{\prime *}, \ \ \forall i \in S$
1: Initialization: $l = 1, l_n = 1$
2: MPC$_c$ solves the MP (9), obtaining $\boldsymbol{u}_c^{\prime l}$ and z^l
3: MPC$_c$ broadcasts $\boldsymbol{u}_c^{\prime l}$ to local controllers MPC$_i$, $\forall i \in S$
4: All MPC$_i$ solve (in parallel) their primal subproblem i, obtaining $\boldsymbol{u}_i^{\prime l, l_n}$
5: **if** $\left| \boldsymbol{u}_i^{\prime l, l_n} - \boldsymbol{u}_i^{\prime l, l_n - 1} \right|_\infty \leq \epsilon', \ \ \forall i \in S$, checked by MPC$_c$ (and $l_n \leq l_{nmax}$)
then
6: All MPC$_i$ solve (in parallel) their dual subproblem i and send their solution, $\tilde{\boldsymbol{p}}_i^l$, to MPC$_c$
7: **else**
8: All MPC$_i$ broadcast $\boldsymbol{u}_i^{\prime l, l_n}$ to all their neighbors $j \in \hbar_i$
9: Update $l_n = l_n + 1$ and Goto step 4
10: **end if**
11: MPC$_c$ computes the current criterion bounds (10)
12: **if** $\bar{v}^l - \underline{v}^l \leq \epsilon$, checked by MPC$_c$ (and $l \leq l_{max}$) **then**
13: $\boldsymbol{u}_c^{\prime *} = \boldsymbol{u}_c^{\prime l}$ and $\boldsymbol{u}_i^{\prime *} = \boldsymbol{u}_i^{\prime l, l_n}, \ \ \forall i \in S$, Stop
14: **else**
15: MPC$_c$ updates the constraints of the MP (adding the new Benders' cut), $l = l + 1$ and Goto step 2
16: **end if**

Weather conditions measured from a geographical location during a previous year were included as part of the simulation. Pricing of electricity and natural gas were assumed to be fixed throughout the day.

Results were compared to a centralized MPC, a decentralized MPC and independent PI loops for the zones. The utility cost resulting from the distributed control approach matched the that from the centralized strategy at 0.79 USD/day, whereas the PI loop implementation reached a cost of 1.06 USD/day. The disadvantage to this distributed control scheme, however, is that the distributed agents relied on computation and inputs from the central coordinator.

In the previous cases visited, the MPC functioned in place of the zone controller. However, the existing building automation control network can be leveraged with the MPC transmitting steady-state targets to the local zone PI controllers. The local zone PI controllers track the target set by a dedicated model predictive controller. In this way, communication occurs between the MPCs, sparing the PI controllers from communicating. For plant-wide optimization, a cost function which accounts for the controller's effect on its upstream and downstream neighbors is proposed [27].

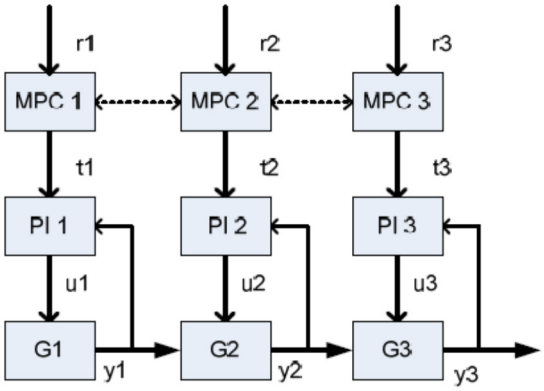

Figure 21 - Network topology with high-level MPC and low-level zone PI control for neighbor communication DMPC [27]

The general form cost function used by each controller in calculating a temperature setpoint is made up of three terms.

$$J_i = f_i(u_i, d_i, r_i) + g_i(y_{i+1}, y_{i-1}, u_i, d_i, r_i) + h_i(y_i)$$

The first term, f_i, is the cost of the individual plant, which would be the same for a decentralized optimization. The second term, g_i, represents the cost impact from the upstream and downstream neighbors. The term, h_i, is the cost that the plant causes to its upstream and downstream neighbors. Within these terms, y_i, r_i, d_i, and u_i, which represent the current state measurement, reference setpoint, disturbance signal and control input, respectively, are considered.

The cost function for the entire system is given by [27]:

$$J = \sum_{i=1}^{3} J_i = \sum_{i=1}^{3} e_i^T Q_i e_i + u_i^T S_i u_i$$

$$\begin{aligned} e_i &= r_i - y_i \\ y_i &= C_i \left(I - A_i\right)^{-1} B_i u_i + C_i \left(I - A_i\right)^{-1} G_i y_{i-1} \\ &= M_i u_i + N_i y_{i-1} \end{aligned}$$

Specifically, the quadratic cost function optimized by each controller is given by:

$$J_i = \underbrace{e_i^T Q_i e_i + u_i^T S_i u_i}_{f_i + g_i} + \underbrace{y_i^T T_i y_i + t_i^T y_i}_{h_i}$$

Where T_i and t_i weight the impact plant *i* has on the other plants. These weights are determined when the neighboring controller communicates the cost impact by plant, ***i***.

A simulation over an 8-hour workday during the summer was run. The plant-wide system developed consisted of four individual rooms, all of which exchanged heat with the hallway and outside air. The static optimizer determined the optimal temperature setpoint to transmit to the zone PI-controller, which regulated the room temperature with the zone cooling capacity. The hallway is assumed to have its own air-conditioner, maintaining 28°C in the space. A depiction of the building model is shown in Figure 16.

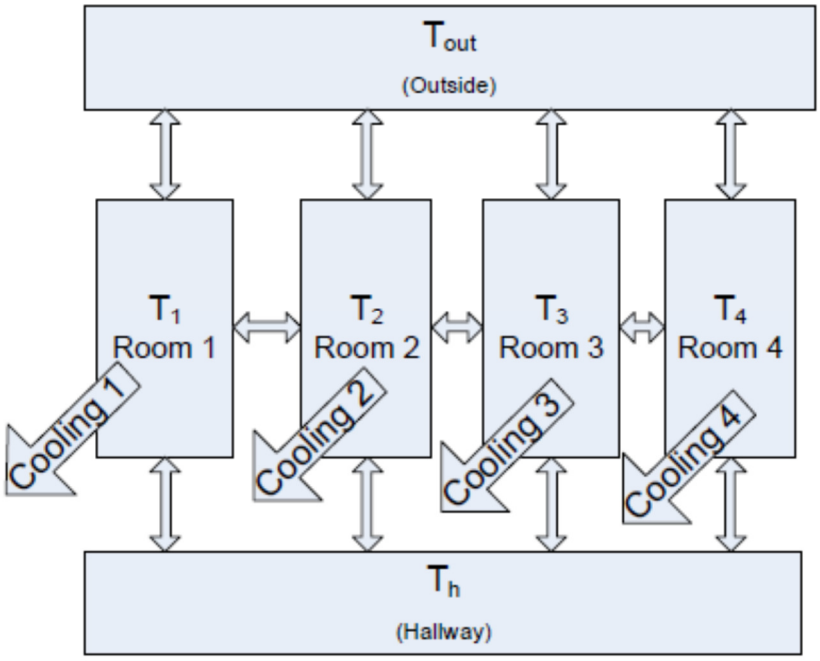

Figure 22 - Building thermal model developed for testing the neighbor-communication DMPC (NC-DMPC) approach [27]

The simulation study entailed subjecting each zone to different magnitudes of thermal disturbance. A run of 2-iterations per step and 10-iterations per step among MPCs was tried. In both cases, the algorithm showed to have acceptable tracking of the centralized MPC, except the 2-iteration DMPC struggles with handling step disturbances.

Chapter 3: DMPC for Demand Response

3.1 Model Development

"…all models are wrong, but some are useful" – George E.P. Box

There are a number of thermal modeling packages available for modeling HVAC system dynamics in controlled environments. Transys, Dymola, Energy Plus and SimBAD are examples of the more sophisticated modeling tools. However, models developed from these tools are useful for architects, engineers and researchers to analyze energy use and thermal efficiencies of varying building materials, loads, floor plans and HVAC system configurations. For the purposes of studying control, a model that sufficiently captures the dynamics of thermal energy transfer through the building envelope and between zones within the building is adequate [14], [28].

Whether the model is generated in a sophisticated modeling package or constructed from first principles governing equations, discrepancies between the model and the actual plant are certain to exist. There is no model that will perfectly represent the dynamics of the actual plant, so a reasonable amount of error is acceptable. In fact, analysis of a system using a linear, time-invariant model enables simplicity without sacrificing valuable information. The use of linear models to represent dynamics decreases computational effort [18]. Furthermore, the state feedback will enable

the controller to adjust for model errors with system identification and state estimation [29].

The models used in this study were derived from considering the system of zones as a network of resistors and capacitors [9], [18], [22], [30] and [31]. The resulting system of linear, first-order differential equations describes the governing behavior of the overall system. The thermal resistance represents the building envelope and zone envelopes. The capacitor corresponds to the thermal mass in the space, such as furniture and construction materials (drywall, cement block, etc…). The total mass is considered as a lumped capacitance.

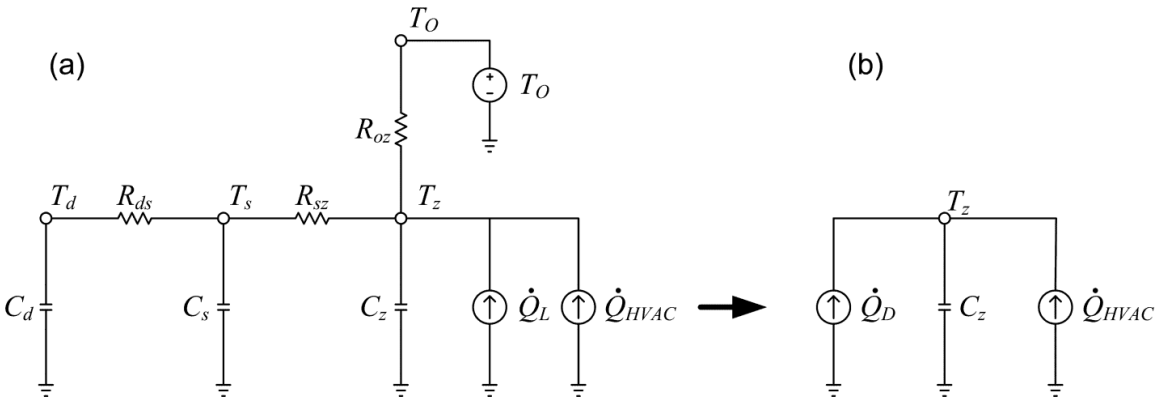

Figure 23 - Simple RC network describing the thermal energy transfer into and out of the zone: (a) Full Model; (b) Reduced model considering heat transfer into or out of the zone as a slowly-moving disturbance

The model simplifies to a zone temperature, T_z, and the thermal capacitance, C_z, of the zone. The energy balance is maintained between the slowly-moving disturbance $\dot{Q}_D$and the removal of the heat by the HVAC system, $\dot{Q}_{HVAC}$.

From the zone model, a mathematical representation of the heat transfer can be formulated using the following fundamental relationships [30]. Equation 1 establishes the relationship between thermal energy transfer in or out of a fixed mass and the temperature of such mass. Equation 2 governs the rate of thermal energy transfer due to a temperature difference across a medium.

$$\dot{T} = \frac{1}{C}[\dot{q}_{in}(t) - \dot{q}_{out}(t)] \qquad (1)$$

$$\dot{q}(t) = \frac{1}{R}[T_1(t) - T_2(t)] \qquad (2)$$

The zone temperature in the space is controlled by a PI controller. $\dot{Q}_{HVAC}$ is modeled as being the output of the PI controller, which is removes heat from the space. The rate of change of the zone temperature is given by:

$$C_z\dot{T}_z = K_q\left[K_p\left(T_{sp} - T_z\right) + K_I I\right] + \dot{Q}_D \qquad (3)$$

The integral term is given by:

$$\dot{I} = T_{sp} - T_z \qquad (4)$$

Where T_{sp} represents the zone temperature setpoint issued by the MPC. K_p and K_I represent the proportional and integral gains, respectively. K_q is a coefficient that converts PI output to cooling power.

The cooling of the space is performed by heating water through a coil. The power required to cool the water at the chiller and cooling tower is modeled as a transfer function with a second-order denominator and first-order numerator. Two time-constants are accounted for in the denominator. One time constant represents the transport delay, and the second time constant represents the mass of the water.

$$\ddot{P} + (\tau_1 + \tau_2)\dot{P} + (\tau_1\tau_2)P = P_{ss} \qquad (5)$$

P_{ss} is the steady-state power transfer at the coil through the COP of the chiller.

The variable, T_s, represents the temperature of the shallow mass in the space. The shallow mass includes the furniture, drywall and framing. Its temperature with respect to time is modeled with the following relationship:

$$\dot{T}_s = \left(1 - \frac{1}{R_{ds}C_s} - \frac{1}{R_{sz}C_s}\right)T_s + \left(\frac{1}{R_{sz}C_s}\right)T_z + \left(\frac{1}{R_{ds}C_s}\right)T_d \qquad (6)$$

Combining (3) - (5), the change in the zone temperature is described by:

$$\dot{T}_z = \left(\frac{1}{R_{ds}C_s}\right)T_s + \left(1 - \frac{1}{R_{sz}C_z} + \frac{K_p}{C_z}\right)T_z - \left(\frac{K_p}{C_zT_i}\right)I + \left(\frac{1}{C_z}\right)P_{dist} - \left(\frac{K_p}{C_z}\right)T_{sp} + \left(\frac{1}{C_z}\right)\dot{Q} \quad (7)$$

The relationship between the change in power consumed and the zone temperature setpoint is given by:

$$\ddot{P} = \left(-\frac{.2K_p}{\tau_1\tau_2}\right)T_z + \left(\frac{.2K_p}{\tau_1\tau_2}\right)I - \left(\frac{1}{\tau_1\tau_2}\right)P + \left(1 - \frac{1}{\tau_1} - \frac{1}{\tau_2}\right)\dot{P} - \left(\frac{.2K_p}{\tau_1\tau_2}\right)T_{sp} \quad (8)$$

The input heat transfer disturbance and the input power disturbance are characterized by the following relationships:

$$\ddot{Q}_{dist} = .9985\dot{Q}_{dist} + \dot{Q}_{dist\_driver} \quad (9)$$

$$\ddot{P}_{dist} = .9985\dot{P}_{dist} + \dot{P}_{dist\_driver} \quad (10)$$

The full zone model is represented in state space form:

$$\dot{\boldsymbol{x}} = \boldsymbol{Ax} + \boldsymbol{Bu}$$

$$\boldsymbol{y} = \boldsymbol{Cx} + \boldsymbol{Du}$$

The state vector of the system:

$$\boldsymbol{x} = \begin{bmatrix} T_s \\ T_z \\ I \\ P \\ \dot{P} \\ \dot{Q}_{dist} \\ P_{dist} \end{bmatrix}$$

T_s	=	Shallow mass temperature
T_z	=	Zone temperature
P	=	Power usage
$\dot{P}$	=	Derivative of power use
$\dot{Q}_{dist}$	=	Thermal load disturbance
P_{dist}	=	Power disturbance

The input vector is given by:

$$\boldsymbol{u} = \begin{bmatrix} T_d \\ T_{sp} \\ \dot{Q} \\ P_{off} \\ \dot{Q}_{dist\_driver} \\ P_{dist\_driver} \end{bmatrix}$$

T_d	=	Deep mass temperature
T_{sp}	=	Temperature setpoint
$\dot{Q}$	=	Thermal energy input
P_{off}	=	Power offset
$\dot{Q}_{dist\_driver}$	=	Thermal energy disturbance input
P_{dist_driver}	=	Power disturbance input

$\boldsymbol{A}$ =

$$\begin{bmatrix} 1-\frac{1}{R_{ds}C_s}-\frac{1}{R_{sz}C_s} & \frac{1}{R_{sz}C_s} & 0 & 0 & 0 & 0 & 0 \\ \frac{1}{R_{sz}C_z} & 1-\frac{1}{R_{sz}C_z}+\frac{K_p}{C_z} & -\frac{K_p}{C_zT_i} & 0 & 0 & 0 & \frac{1}{C_z} \\ 0 & -1 & 1 & 0 & 0 & 0 & 0 \\ 0 & 0 & 0 & 1 & 1 & 0 & 0 \\ 0 & -\frac{0.2K_p}{\tau_1\tau_2} & \frac{0.2K_p}{\tau_1\tau_2T_i} & -\frac{1}{\tau_1\tau_2} & 1-\frac{1}{\tau_1}-\frac{1}{\tau_2} & 0 & 0 \\ 0 & 0 & 0 & 0 & 0 & .9985 & 0 \\ 0 & 0 & 0 & 0 & 0 & 0 & .9985 \end{bmatrix}$$

$$\boldsymbol{B} = \begin{bmatrix} \frac{1}{R_{ds}C_s} & 0 & 0 & 0 & 0 & 0 \\ 0 & \frac{-K_p}{C_z} & \frac{1}{C_z} & 0 & 0 & 0 \\ 0 & 1 & 0 & 0 & 0 & 0 \\ 0 & 0 & 0 & 0 & 0 & 0 \\ 0 & \frac{-0.2K_p}{\tau_1\tau_2} & 0 & 0 & 0 & 0 \\ 0 & 0 & 0 & 0 & 1 & 0 \\ 0 & 0 & 0 & 0 & 0 & 1 \end{bmatrix}$$

$$\boldsymbol{C} = \begin{bmatrix} 0 & 1 & 0 & 0 & 0 & 0 & 0 \\ 0 & 0 & 0 & 1.9 & 0 & 0 & 0.2 \end{bmatrix}$$

$$\boldsymbol{D} = \begin{bmatrix} 0 & 0 & 0 & 0 & 0 & 0 \\ 0 & 0 & 0 & 1 & 0 & 0 \end{bmatrix}$$

The model can be used to represent either zone by manipulation of the thermal resistances of the walls and thermal capacitance values of each zone. Selecting appropriate values for the building parameters such as floor area of each zone and the R-values of the construction materials fixes the thermal capacitance and thermal resistance values, respectively.

Values for the various construction materials are found in texts or vendor specifications. For the building in this model, it is reasonable to assume that the exterior wall is constructed of split-faced concrete block, insulated steel-studs and interior gypsum board. This wall construction is consistent with what would be expected for commercial building construction [32]. Appropriate values of heat transmission coefficients for the windows, built-up roofing and slab are found in, [33, p. 145], [33, p. 145] and [33, p. 150], respectively. Building dimensions are shown in table 3. Thermal loading characteristics are presented in table 4.

Exterior Wall Construction	
Wall Height	3.66 m
Wall Area	4212.0 m^2
Wall U-Value	.119 [W/m^2K]
Windows Area	2268.0 m^2
Windows U-Value	2.90 [W/m^2K]
Built-Up Roof	
U-Value	.196 [W/m^2K]
Zone 1	
Floor Area	3,403.0 m^2
Zone 2	
Floor Area	15,129.0 m^2
Slab	
U-Value	1.75 [W/mK]
Perimeter	540.0 m

Table 5 – Modeled building parameters for simulation

The step response of temperature for zones 1 and 2 are shown in Figure 24 and Figure 25, respectively. Initially, the temperature in the space is 25°C, and a setpoint of 20°C is issued. The outdoor air temperature is not a factor, and neither zone is subject to internal thermal loading.

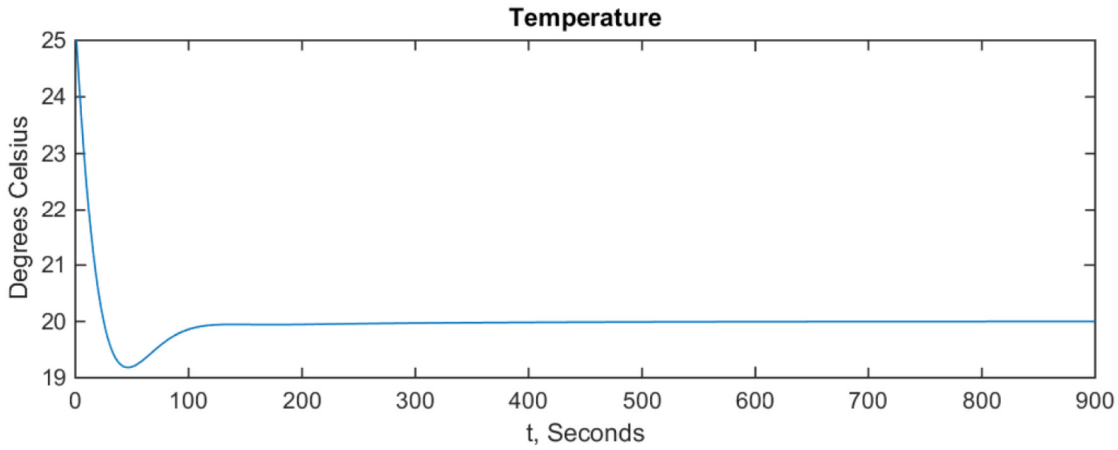

Figure 24 - Zone 1 response to temperature setpoint

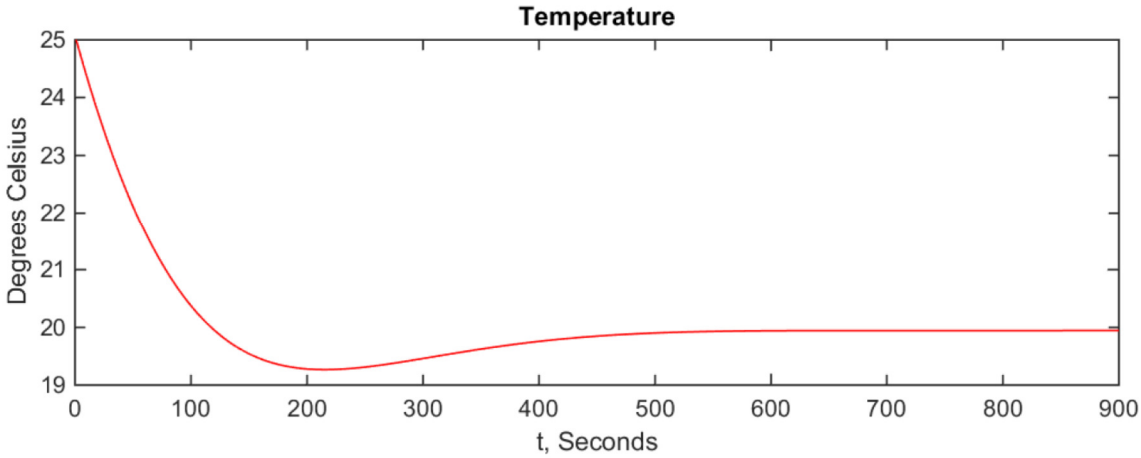

Figure 25 - Zone 2 response to temperature setpoint

The power required to cool zone 1 from 25°C to 20°C is shown in Figure 26. Similarly, the power required to cool zone 2 from 25°C to 20°C is shown in Figure 27.

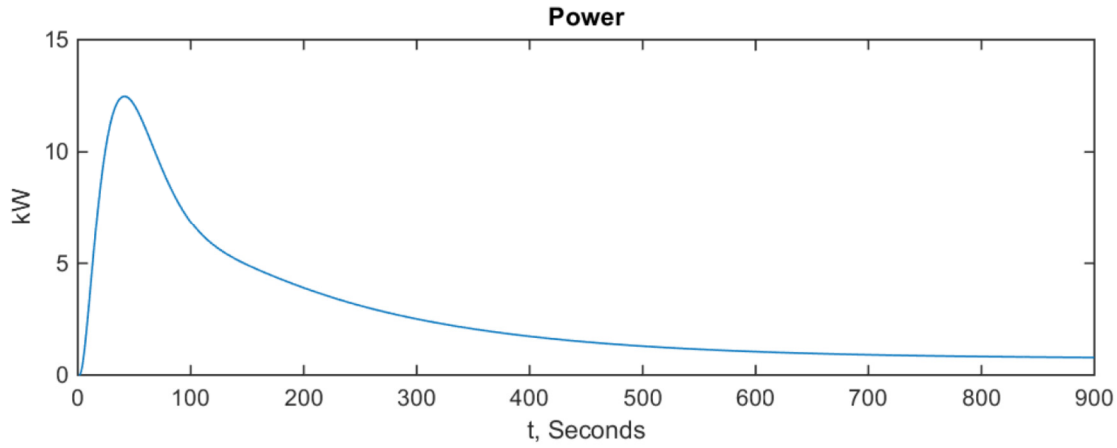

Figure 26 - Zone 1 power profile

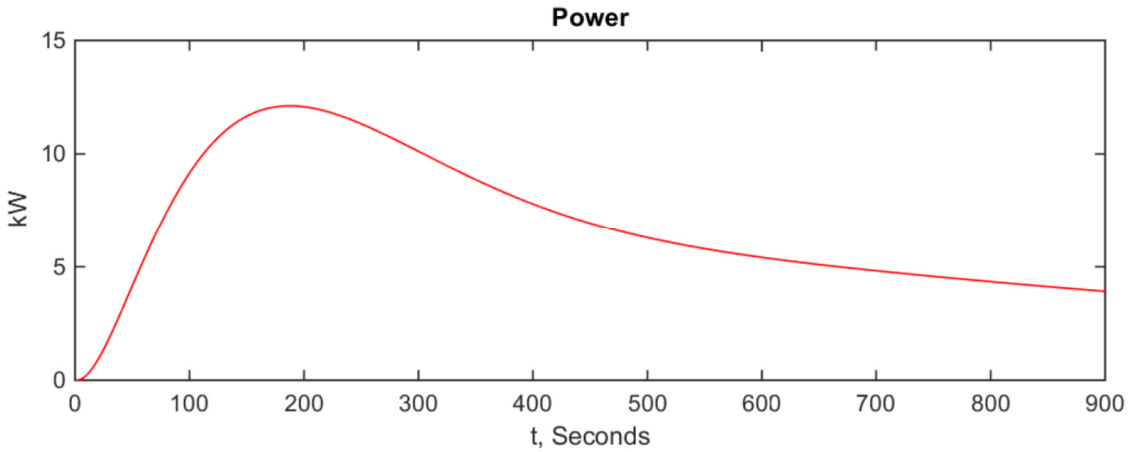

Figure 27 - Zone 2 power profile

Zone 1 exhibits a faster response to a step input than zone 2. Lowering the temperature in zone 1 from 25°C to 20°C requires energy use at an average rate of 2.71 kW for a total of 0.67 kW-h. Comparatively, lowering the temperature in zone 2 from 25°C to 20°C requires energy use at an average rate of 6.92 kW for a total of 1.73 kW-h during the 15-minute period.

3.2 Objective Function

The cost function is a linear economic objective function which represents the cost of cooling the zone. The goal of the control system is to optimize economic performance of the two-zone system. Cost is minimized over the prediction horizon subject to the temperature band constraint. The cost function represents the trade-off in cooling the zone at the current time, t, versus the cost of cooling at a future time, t + k. Inherent in the cost function is the consideration of whether power usage may be deferred until a later point in time, or if more power must be used at the current time to keep the zone temperature within the defined temperature band or to utilize the building mass for the storage of thermal energy which can be discharged at a later point in time.

$$J = \sum_{i}^{i+k-1} EC(i) * P_1(i) + \sum_{i}^{i+k-1} EC(i) * P_2(i)$$

$$\min J \quad \text{s.t.} \begin{cases} T_{min} \leq T_{zone} \leq T_{max} \\ \\ \dot{\boldsymbol{x}}_{\boldsymbol{1}} = \boldsymbol{A_1 x_1} + \boldsymbol{B_1 u_1} \\ \boldsymbol{y_1} = \boldsymbol{C_1 x_1} + \boldsymbol{D_1 u_1} \\ \dot{\boldsymbol{x}}_{\boldsymbol{2}} = \boldsymbol{A_2 x_2} + \boldsymbol{B_2 u_2} \\ \boldsymbol{y_2} = \boldsymbol{C_2 x_2} + \boldsymbol{D_2 u_2} \end{cases}$$

where T_{min} and T_{max} are the minimum and maximum allowable zone temperature setpoints that can be issued by the MPC, respectively.

The plant cost function is the sum of the energy cost, EC, from the current interval, i, through k intervals into the future. In both the centralized and distributed approaches presented, the economic performance of the plant is optimized over a horizon of 30, 15-minute intervals. Each 24-hour period consists of 96, 15-minute intervals, so the horizon is roughly one third of the course of a day. This is sufficient length for predictions to be made without sacrificing computing performance (i.e., as the horizon increases, more iterations are required during the optimization calculation).

3.3 The Centralized MPC Approach

Zones 1 and 2 are thermally coupled, meaning their zone temperatures can affect the other. The interaction between the two zones is described with the following relationships [25]:

$$q_1 = \alpha(T_2 - T_1) \quad (11)$$

$$q_2 = \alpha(T_1 - T_2) \quad (12)$$

Where α is the coupling strength, and T_1 and T_2 represent the temperatures of zone 1 and zone 2, respectively. The coupling strength may be thought of as the inverse of thermal resistance. The higher the coupling strength, the greater the thermal influence each zone exerts on the other.

The outer layer is the real-time optimization layer (RTO), responsible for optimizing the economic performance of the plant. The optimal zone temperature setpoint trajectory is computed at this level. The first step of the setpoint trajectory is sent to the lower-level PI controller. The outer layer samples every 15 minutes, which coincides with the frequency of utility pricing updates. The lower level PI algorithm runs at a frequency of 1 Hz for the purpose of disturbance rejection.

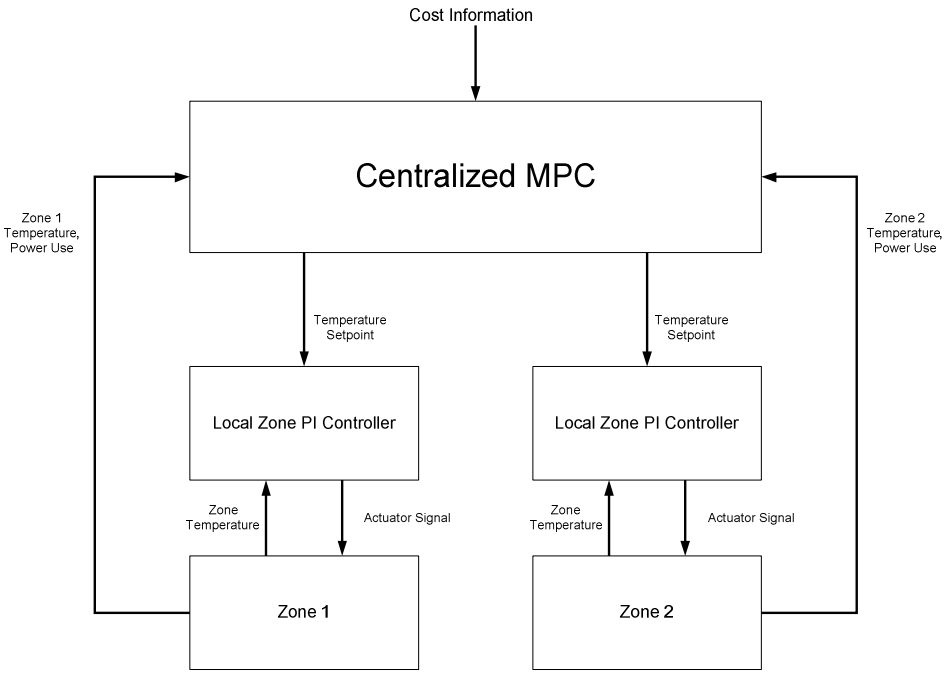

Figure 28 – Centralized MPC implementation

The RTO calculation is handled with the fmincon function in Matlab. The function iterates through the zone models with the setpoint trajectory as the input. When the least-cost is reached, the corresponding trajectory is used. The first element in the optimal zone temperature trajectory is transmitted as a setpoint to the zone PI controller.

3.4 Distributed MPC System Architecture

The RTO layer is divided such that there is a dedicated MPC for each zone, as depicted in Figure 29. This approach to control architecture is readily used in processes currently [34].

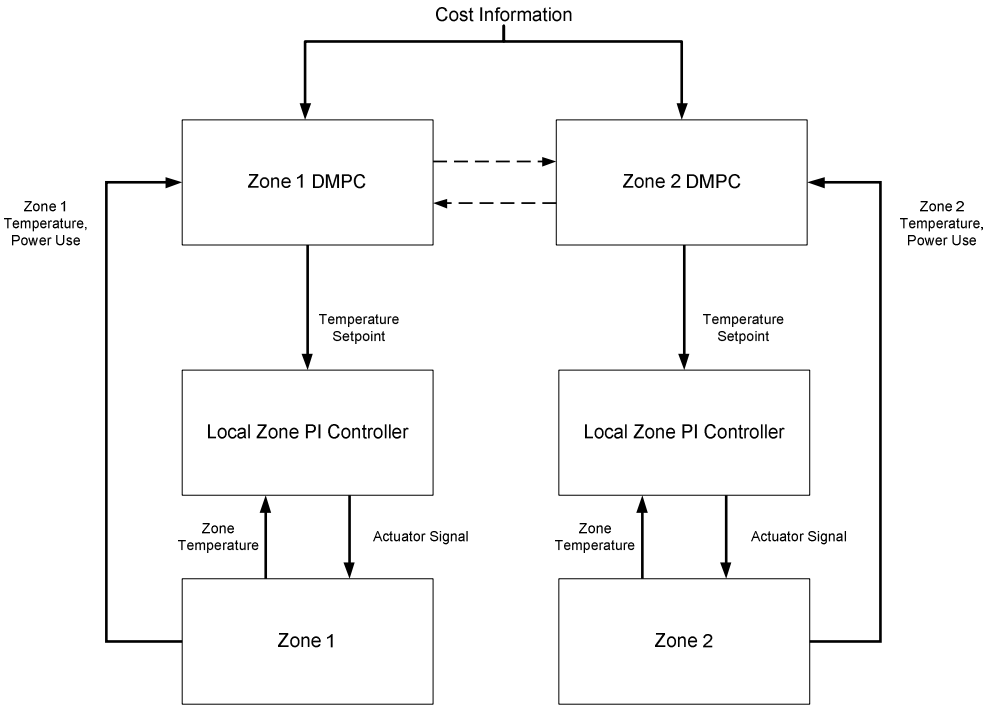

Figure 29 – Cascaded DMPC Architecture

3.5 Distributed MPC Algorithm

The distributed MPC algorithm analyzed in this study includes 2 layers for control of the plant. Similar to the centralized control, there exists a RTO layer that determines the temperature setpoint trajectory which costs the least over the horizon. The temperature setpoint is transmitted to a lower-level PI controller. Communication occurs between the distributed controllers to share anticipated temperature setpoint trajectories. The algorithm used in this thesis is based off of the agent negotiation principle [35]. This sharing of information is useful so that neighboring agents adjust for neighboring disturbances, and in turn the disturbance each causes to other agents' intended paths. In this way, after each calculation update, each individual controller can update its planned course of action based on the anticipated trajectories of other controllers.

The algorithm executes as follows:

1. Starting at $T_{sp1} = 25$ and $T_{sp2} = 25$, controller 1 produces $T_{sp1,1}(k \cdots k+n-1)$ and the temperature trajectory of zone 2 for minimum cost, $T_{sp2,1}(k \cdots k+n-1)$.

2. Controller 2 checks controller 1 output and produces $T_{sp2,2}(k \cdots k+n-1)$ from starting point, $T_{sp2,1}(k \cdots k+n-1)$ and proposed disturbance, $T_{sp1,1}(k \cdots k+n-1)$. The first cost is recorded.

3. Controller 1 produces $T_{sp1,2}(k \cdots k+n-1)$ from starting point, $T_{sp1,1}(k \cdots k+n-1)$ and proposed disturbance, $T_{sp2,1}(k \cdots k+n-1)$. The second cost is recorded.

4. Controller 1 calculates $T_{sp1,3}(k \cdots k+n-1)$ from starting point, $T_{sp1,1}(k \cdots k+n-1)$ and proposed disturbance, $T_{sp2,2}(k \cdots k+n-1)$. The third cost is recorded.

5. The first elements of the temperature trajectories resulting in the least cost are transmitted to the respective PI controllers.

6. On the next (alternate) iteration: Starting at $T_{sp1} = 25$ and $T_{sp2} = 25$, controller 2 produces $T_{sp2,1}(k \cdots k+n-1)$ and the temperature trajectory of zone 1 for minimum cost, $T_{sp1,1}(k \cdots k+n-1)$.

7. Controller 1 checks controller 2 output and produces $T_{sp1,2}(k \cdots k+n-1)$ from starting point, $T_{sp1,1}(k \cdots k+n-1)$ and proposed disturbance, $T_{sp2,1}(k \cdots k+n-1)$. The first cost is recorded.

8. Controller 2 produces $T_{sp2,2}(k \cdots k+n-1)$ from starting point, $T_{sp2,1}(k \cdots k+n-1)$ and proposed disturbance, $T_{sp1,1}(k \cdots k+n-1)$. The second cost is recorded.

9. Controller 2 calculates $T_{sp2,3}(k \cdots k+n-1)$ from starting point, $T_{sp2,1}(k \cdots k+n-1)$ and proposed disturbance, $T_{sp1,2}(k \cdots k+n-1)$. The third cost is recorded.

10. The first elements of the temperature trajectories resulting in the least cost are transmitted to the respective PI controllers.

11. Next calculation starts at step 1. The controller initializing calculations alternates at each 15-minute interval.

3.6 Results

For all simulations, the values of T_{min} and T_{max} were set at 20°C (68°F) and 25°C (77°F), respectively. The value of the coupling constant, alpha, is set at 7.0kW/°C, representing the thermal transmission by conduction through an interior wall. The outdoor air temperature profile is shown in Figure 30. The data used were recorded on August 30, 2010 at the San Francisco International Airport [36].

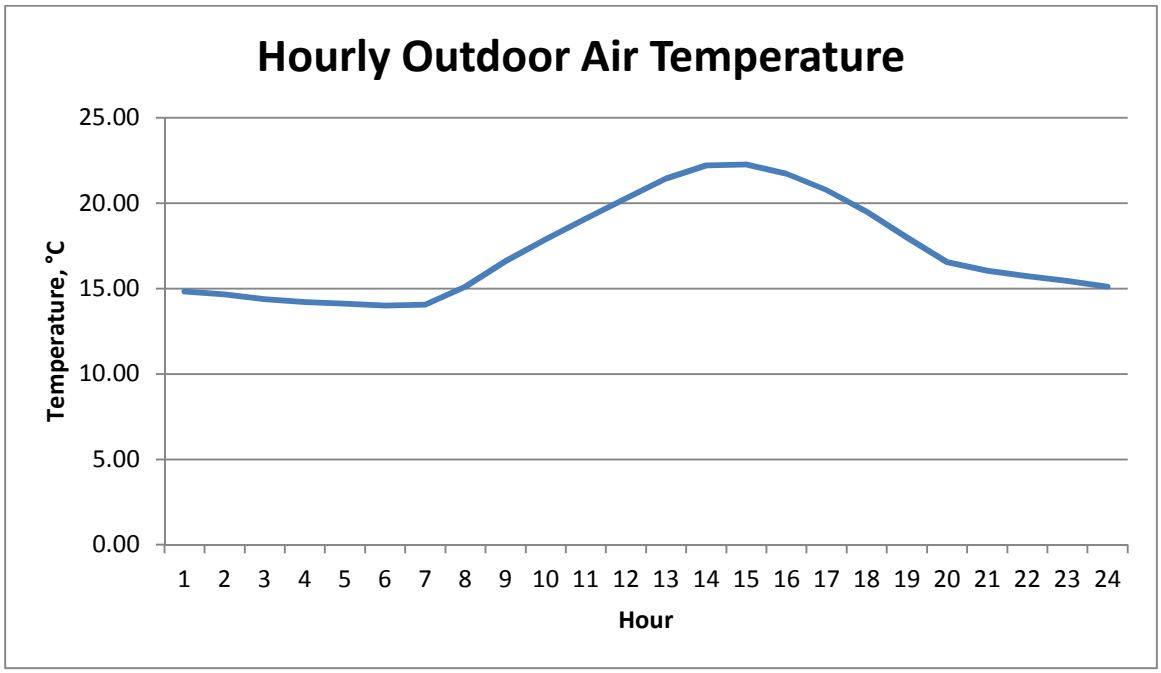

Figure 30 - Outdoor air temperature profile for simulation

The thermal load generated within the space is a sum of the equipment (computers, machines, etc...), lighting and occupants. Both zones are assumed to have a moderate density occupancy, based on the area of the space [32]. The difference in

their loading is due to the time of day at which the loads peak and the duration of occupancy. It is assumed that in either zone, there will be a dip in power demand in the middle of the day due to people stepping out of the workspace for lunch.

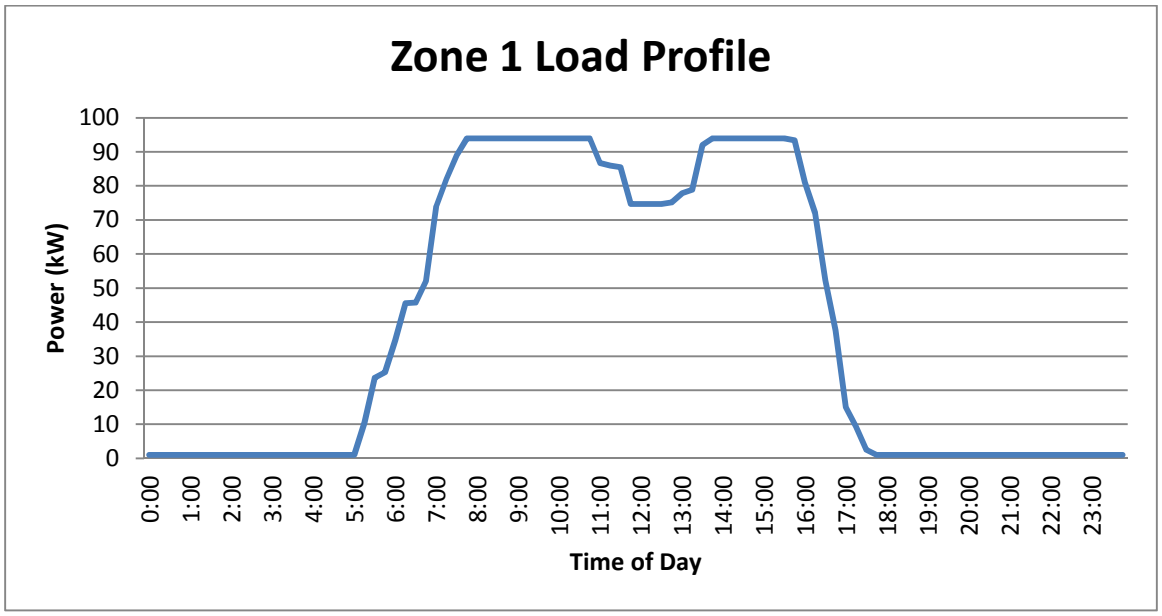

Figure 31 - Zone 1 load profile

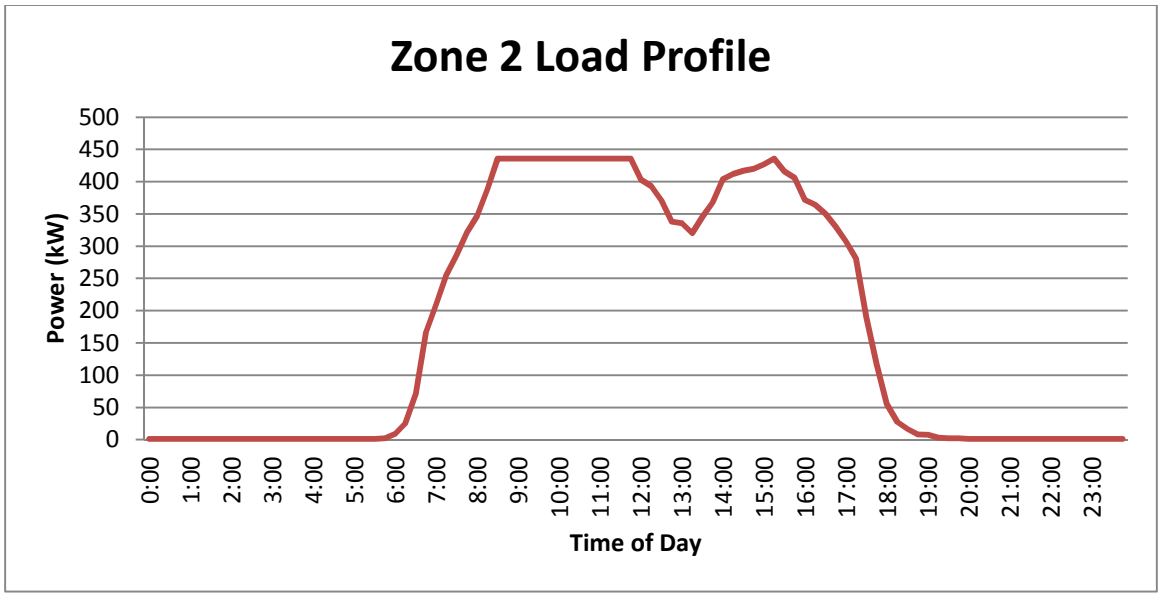

Figure 32 - Zone 2 load profile

3.6.1 Decentralized, PI-Control Performance

The following results were obtained from simulations. Figure 33 and Figure 34 show the PI-only control performance for zone 1 and zone 2, respectively. The temperature setpoint is maintained at 25°C through the entire simulation. The choice of setpoint represents minimum energy consumption, as it is at the top end of the comfort band.

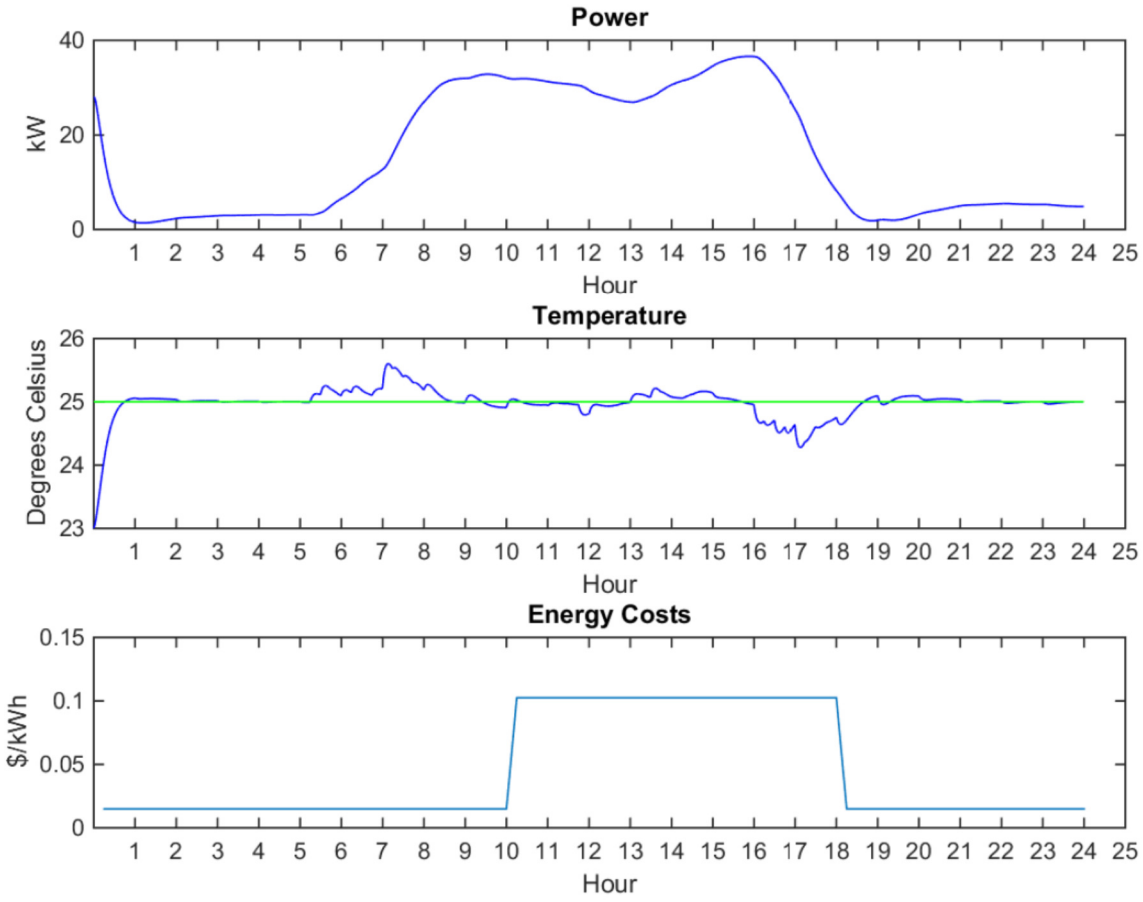

Figure 33 - Zone 1 PI-Only Control

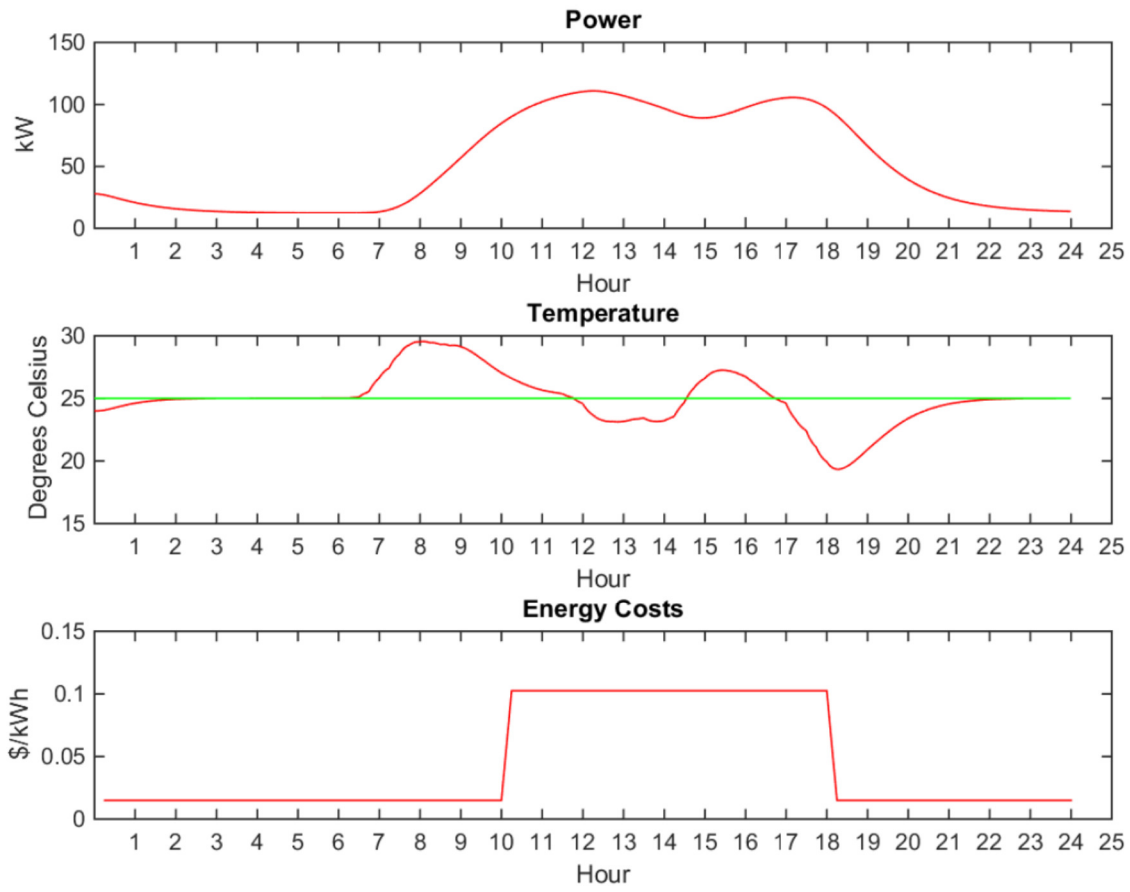

Figure 34 - Zone 2 PI-Only Control

The energy costs for both zones totaled $462.52. Zone 1 remained under control reasonably well, while zone 2 faced some challenges. This is not due to the PI controller; instead it is a product of the nature of the zone dynamics. Zone 1 is a smaller zone and therefore elicits a quicker response to load disturbances. Zone 2 on the contrary is a larger space and elicits a slower response to load disturbances.

3.6.2 Centralized MPC Performance

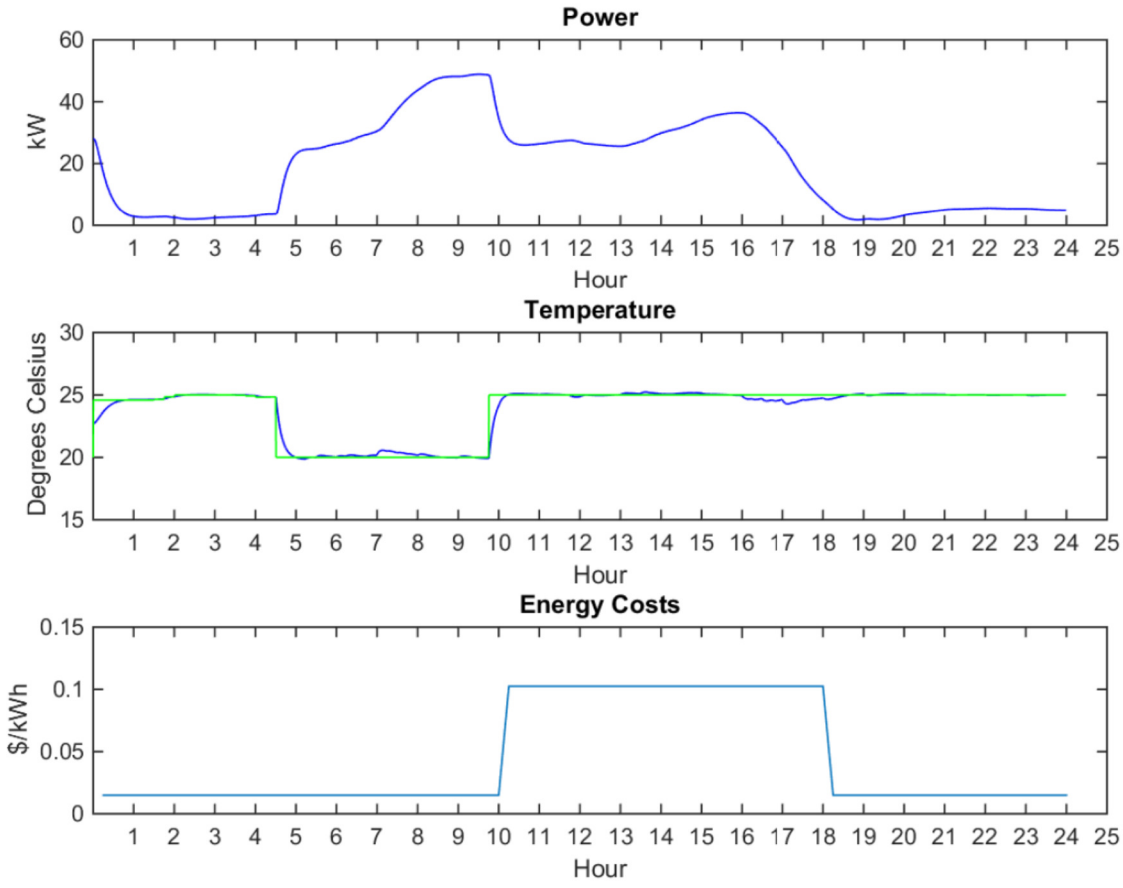

Figure 35 - Centralized Control, Zone 1 Performance

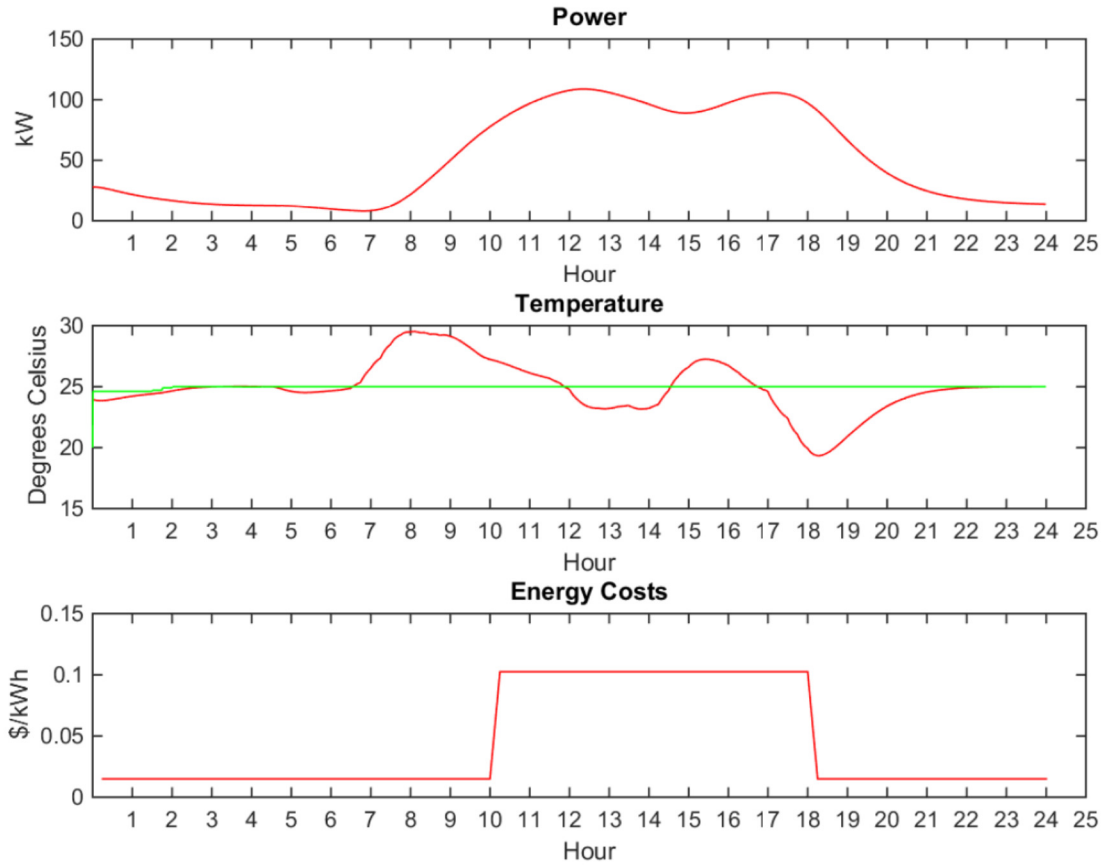

Figure 36 - Centralized Control, Zone 2 Performance

The centralized MPC showed to cut the energy costs down to $456.48 per day.

3.6.3 Distributed MPC Performance

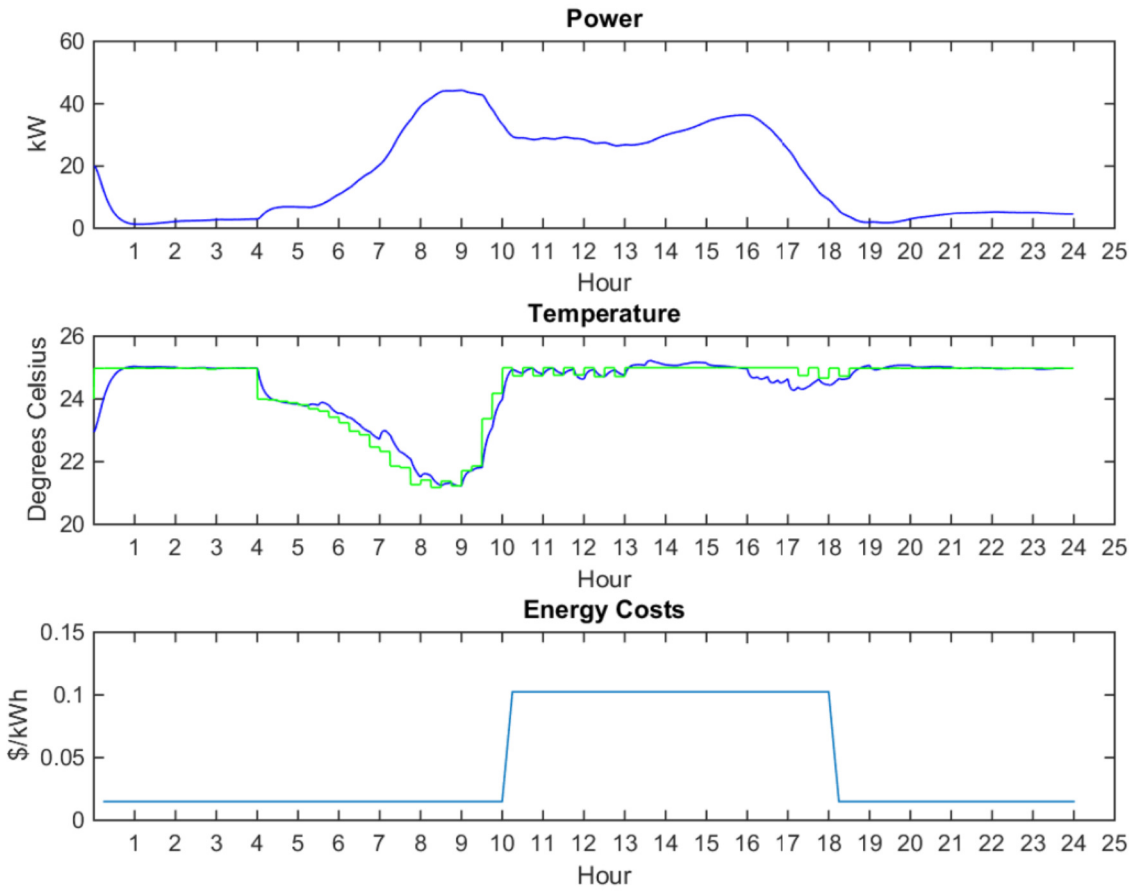

Figure 37 - Zone 1 DMPC Performance

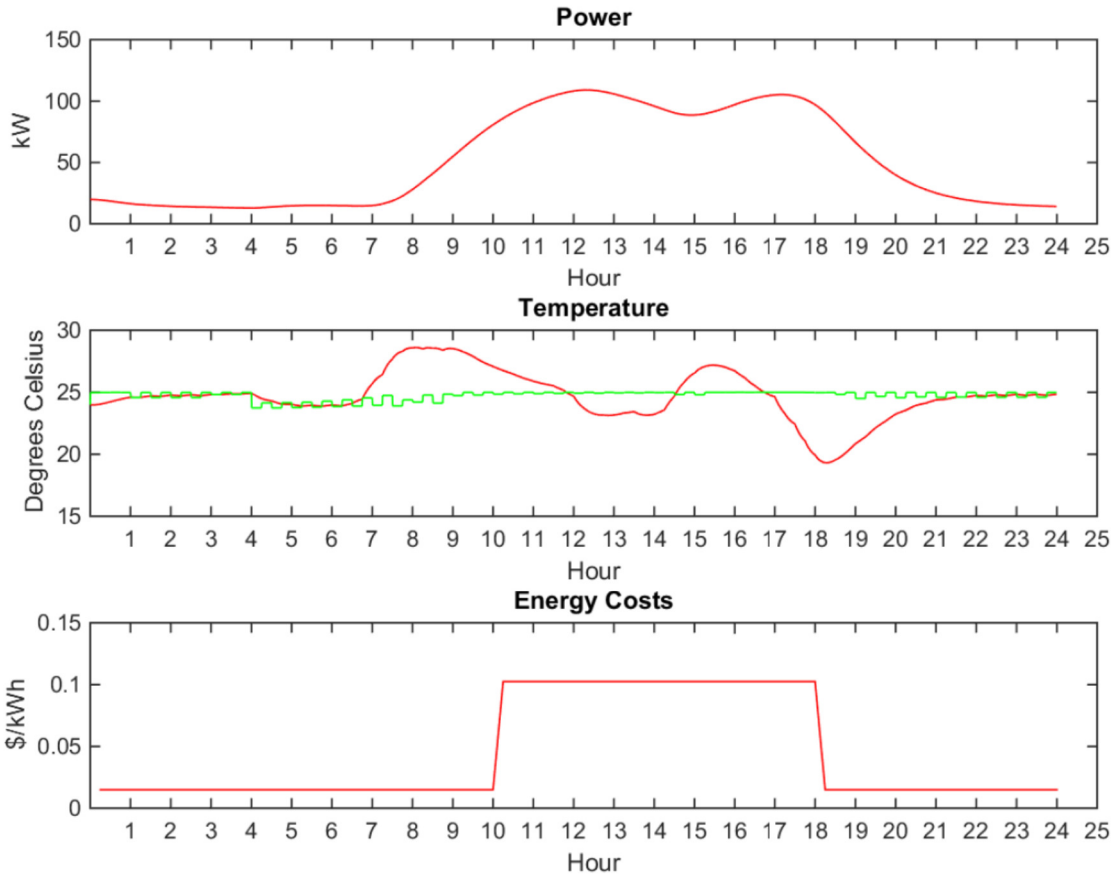

Figure 38 - Zone 2 DMPC Performance

The distributed MPC scheme resulted in a cost of $457.38 per day. This is closely in line with the result of the centralized MPC scheme. The mass of zone 2, and therefore its slower response challenged the control function (both PI and MPC) to handle the load disturbance. In either case, the centralized control approach and the distributed control approach showed to reduce the energy costs for the building modeled. The advantage that the distributed approach has is that the computing effort is shared between two controllers optimizing their own objective function

and sharing the outcomes with the other controller before a final temperature setpoint trajectory is followed. The centralized control required that the entire plant be solved at each interval. This increases the computing effort for systems with greater than one zone.

Chapter 4: Conclusions & Future Work

4.1 Conclusion

Within the realm of MPC applied to HVAC space, there are subclasses of similar algorithms and objectives. The implementations tested are categorized as centralized or distributed. Within the classes of implementation are the various forms of objective functions, either intended to minimize energy consumption or energy cost. Simulations highlighting the reduction of utility costs for an air-side HVAC system in the presence of real-time energy pricing have been presented. The strategy of pre-cooling the building mass ahead of energy price hikes is demonstrated for a two-zone, thermally coupled system. Each zone is a different size and therefore represents a different capacity for thermal storage. The system leverages the existing building construction without the construction of chilled water storage tanks.

The distributed MPC algorithm demonstrated to have favorable performance relative to the centralized MPC benchmark. Furthermore, both control algorithms proved to save cost over the standard PI-only controllers. It is also demonstrated that the PI controllers operated with the zone temperature constraint active, thus using the least amount of energy. Therefore, this illustrates the point that minimizing energy consumption is not necessarily the same as minimizing cost.

While this study has found that the cost savings achieved for the scenario presented is on the order of dollars per day, it is entirely possible that a higher savings potential exists with chilled water storage. However, it is important to consider that a significant up-front investment for the scenario presented is not needed. The existing building control infrastructure may be leveraged, and the construction of water storage tanks is not necessary.

4.2 Direction for Future Research

Most importantly from this study, the examination of the initial capital investment versus return on investment should be conducted for both the air-side system and the chilled water storage system. This analysis will be useful in determining which route is best for the building planning.

The extension to systems greater than two zones should be investigated. It would be best to examine larger systems with controller hardware running against a simulated plant model. The reason for this is that simulating larger systems on a desktop PC greatly extend the amount of time to complete a single simulation if the PC does not run out of memory while doing so. There may be advantages to simulating a 7-zone system, with zones having any combination of thermal mass.

Along the lines of computing power, a simpler model of the relation between power use and the steady-state temperature in the space should be developed. The amount of computing time required to churn through the model and optimize the plant over the horizon may be reduced from the use of a simpler model.

Lastly, after the software has undergone testing, this algorithm along with variations of it should be field-tested in the scenarios this control scheme was designed for. A full system test will help to identify weaknesses not uncovered in simulation trials. When it is time for this control system to be put to the test on a live plant, it is essential that necessary sensor readings such as power use and zone temperatures are gathered for a complete comparison of the field results to those obtained through software simulation.

REFERENCES

[1] U.S. Energy Information Administration, "Annual Energy Outlook," United States Dept. of Energy, Washington, D.C., 2014.

[2] U.S. Dept. of Energy, "Benefits of Demand Response in Electricity Markets and Recommendations for Achieving Them," U.S. Dept. of Energy, Washington, D.C., 2006.

[3] M. Yalcintas, W. T. Hagen and A. Kaya, "An analysis of load reduction and load shifting techniques in commercial and industrial buildings under dynamic electricity pricing schedules," *Energy and Buildings,* vol. 88, pp. 15-24, 2015.

[4] U.S. Dept. of Energy, "A National Assessment of Demand Response Potential," U.S. Dept. of Energy, Washington, D.C., 2009.

[5] Tiax, LLC, "Energy Impact of Commercial Building Controls and Performance Diagnostics: Market Characterization, Energy Impact of Building Faults and Energy Savings Potential," U.S. Dept. of Energy, Washington, D.C., 2005.

[6] J. E. Braun, "Reducing Energy Costs and Peak Electrical Demand through Optimal Control of Building Thermal Storage," *ASHRAE Transactions,* vol. 96, no. 2, pp. 876-888, 1990.

[7] Energy Star, "Air-Side Economizer," [Online]. Available: https://www.energystar.gov/index.cfm?c=power_mgt.datacenter_efficiency_economizer_airside. [Accessed 5 January 2015].

[8] K. H. Ang, G. Chong and Y. Li, "PID Control System Analysis, Design, and Technology," *IEEE Transactions on Control Systems Technology,* vol. 13, no. 4, pp. 559-576, 2005.

[9] K. Ogata, Modern Control Engineering, 4th Ed., Upper Saddle River, NJ: Prentice Hall, 2002.

[10] J. B. Rawlings, D. Angelii and C. N. Bates, "Fundamentals of Economic Model Predictive Control," in *51st IEEE Conference on Decision and Control*, Maui, HI, 2012.

[11] A. Afram and F. Janabi-Sharifi, "Theory and applications of HVAC control systems - A review of model predictive control (MPC)," *Building and Environment,* vol. 72, pp. 343-355, 2014.

[12] P. M. Ferreira, S. M. Silva and A. E. Ruano, "Energy Savings in HVAC Systems Using Discrete Model-Based Predictive Control," in *IEEE World Congress on Computational Intelligence*, Brisbane, 2012.

[13] S. C. Bengea, A. D. Kelman, F. Borrelli, R. Taylor and S. Narayanan, "Implementation of model predictive control for an HVAC system in a mid-size commercial building," *HVAC&R Research,* vol. 20, no. 1, pp. 121-135, 2014.

[14] M. Vasak, A. Starcic and A. Martincevic, "Model predictive control of heating and cooling in a family house," in *MIPRO, 2011 Proceedings of the 34th International Convention*, Adriatic Coast, Croatia, 2011.

[15] J. D. Alvarez, J. L. Redondo, E. Camponogara, J. Normey-Rico, M. Berenguel and P. M. Ortigosa, "Optimizing building comfort temperature regulation via model predictive control," *Energy and Buildings,* vol. 57, pp. 361-372, 2013.

[16] P.-D. Morosan, R. Bourdais, D. Dumur and J. Buisson, "Building temperature regulation using a distributed model predictive control," *Energy and Buildings,* vol. 42, no. 9, pp. 1445-1452, 2010.

[17] S. R. West, J. K. Ward and J. Wall, "Trial results from a model predictive control and optimisation system for commercial building HVAC," *Energy and Buildings,* vol. 72, pp. 271-279, 2014.

[18] M. Maasoumy and A. Sangiovanni-Vincentelli, "Total and Peak Energy Consumption Minimization of Building HVAC Systems Using Model Predictive Control," *IEEE Design & Test of Computers,* pp. 26-35, July/August 2012.

[19] V. M. Zavala, "Real-Time Optimization Strategies for Building Systems," Argonne National Laboratory, Argonne, IL, 2011.

[20] M. Avci, M. Erkoc, A. Rahmani and S. Asfour, "Model predictive HVAC load control in buildings using real-time electricity pricing," *Energy and Buildings,* vol. 60, pp. 199-209, 2013.

[21] J. Ma, J. Qin, T. Salsbury and P. Xu, "Demand reduction in building energy systems based on economic model predictive control," *Chemical Engineering Science,* vol. 67, no. 1, pp. 92-100, 2012.

[22] C.-J. Boo, J.-H. Kim, H.-C. Kim, M.-J. Kang and K. Y. Lee, "Energy Efficient Temperature Control for Peak Power Reduction in Building Cooling Systems," *International Journal of Control and Automation,* vol. 6, no. 6, pp. 105-114, 2013.

[23] J. M. Maestre and R. R. Negenborn, Eds., Distributed Model Predictive Control Made Easy, Dordrecht, Netherlands: Springer, 2014.

[24] S. J. Qin and T. A. Badgwell, "A survey of industrial model predictive control technology," *Control Engineering Practice,* vol. 11, no. 7, pp. 733-764, 2003.

[25] V. Putta, G. Zhu, D. Kim, J. Hu and J. Braun, "A Distributed Approach to Efficient Model Predictive Control of Building HVAC Systems," in *International High Performance Buildings Conference at Purdue*, West Lafayette, IN, 2012.

[26] P.-D. Morosan, R. Bourdais, D. Dumur and J. Buisson, "A distributed MPC strategy based on Benders' decomposition applied to multi-source multi-zone temperature regulation," *Journal of Process Control,* vol. 21, no. 10, pp. 729-737, 2011.

[27] M. S. Elliott and B. P. Rasmussen, "Neighbor-Communication Model Predictive Control and HVAC Systems," in *2012 American Control Conference*, Montreal, 2012.

[28] F. A. Barata, N. Felix and R. Neves-Silva, "Distributed MPC for green thermally comfortable buildings based on an electro-thermal modular approach," in *Conference on Electronics, Telecommunications and Computers*, Lisbon, 2013.

[29] J. B. Rawlings, Model Predictive Control: Theory and Design, Madison, WI: Nob Hill Publishing, LLC, 2013.

[30] C. M. Close, D. H. Frederick and J. C. Newell, Modeling and Analysis of Dynamic Systems, 3rd Ed., New York: John Wiley & Sons, Inc., 2002.

[31] G. F. Franklin, J. D. Powell and A. Emami-Naeini, Feedback Control of Dynamic Systems, Upper Saddle River, NJ: Pearson Higher Education, Inc., 2010.

[32] Kingspan, "Building Science Corporation Report," [Online]. Available: http://www.kingspanpanels.us/kingspanunitedstatesmain/media/pdfDownloads/Sustainability/White%20Papers/Literature/Building-Science-Corporation-Report.pdf. [Accessed 8 April 2015].

[33] F. C. McQuiston, J. D. Parker and J. D. Spitler, Heating, Ventilating, and Air Conditioning Analysis and Design, Hoboken, NJ: John Wiley & Sons, Inc., 2005.

[34] R. Scattolini, "Architectures for distributed and hierarchal Model Predictive Control - A review," *Journal of Process Control,* vol. 19, no. 5, pp. 723 - 731, 2009.

[35] P. D. Christofides, R. Scattolini, D. Munoz de la Pena and J. Liu, "Distributed model predictive control: A tutorial review and future research directions," *Computers and Chemical Engineering,* vol. 51, pp. 21 - 41, 2013.

[36] National Oceanic and Atmospheric Administration, "National Climatic Data Center," [Online]. Available: http://www.ncdc.noaa.gov/cdo-web/datatools/normals. [Accessed 24 April 2015].

[37] C. E. Garcia, D. M. Prett and M. Morari, "Model Predictive Control: Theory and Practice-a Survey," *Automatica,* vol. 25, no. 3, pp. 335-348, 1989.